Single and hybrid organoclay-filled PLA nanocomposites: Mechanical properties, viscoelastic behavior and fracture toughening mechanism

Jefferson Lopes Alves [a], Paulo de Tarso Vieira e Rosa [b], Vera C. de Redondo Realinho [c], Marcelo de Sousa Pais Antunes [c], José Ignacio Velasco [c], Ana Rita Morales [a*]

[a] School of Chemical Engineering, State University of Campinas, Av. Albert Einstein, 500, 13083-852, Campinas-SP, Brazil
[b] Institute of Chemistry, State University of Campinas, P.O. Box 6154, 13083-970, Campinas-SP, Brazil
[c] Department of Materials Science and Engineering, Poly2 Group, Technical University of Catalonia (UPC BarcelonaTech), ESEIAAT, Colom 11, 08222 Terrassa (Barcelona), Spain
[*] Corresponding author: morales@unicamp.br

Abstract

Poly (lactic acid) (PLA) nanocomposites based on single and hybrid organic-modified montmorillonites were previously studied in terms of their morphological, thermal and fire performance. As surfactants of the organoclays influenced the compatibility between the nanofillers and PLA with different degrees of clay platelets dispersion, the present work investigated the effect of these features in the mechanical properties of PLA nanocomposites. PLA nanocomposites specimens were analyzed by dynamic-mechanical-thermal analysis, which pointed out changes in the viscoelastic behavior of the materials by the incorporation of the organoclays, namely the increase of the storage modulus due to polymer chains movements restriction and reinforcement effects associated with the dispersion of the nanofillers. Flexural and impact testing showed that hybrid organo-montmorillonites containing ester ammonium and ethoxylated amine improved PLA's ductility, toughness and impact resistance. This behavior was explained by the high level of compatibility and interaction between the surfactants and PLA chains due to the polar groups in their structures. These organoclays caused a transition on PLA's fracture from brittle to ductile in a way that the toughening mechanism was explained by crazing and multi-shear banding induced by the plasticized interfacial region around these organoclays.

Keywords: clay, composites, mechanical properties

1. Introduction

Poly (lactic acid) (PLA), a biodegradable thermoplastic, has been gaining ground in medical, durable and non-durable consumer applications, due to issues related to sustainability and the environment. PLA is considered safe for human health (low toxicity), according to the US Food and Drug Administration (FDA) (Garlotta, 2001; Ahmed and Varshney, 2011; Armentano et al., 2013; Castro-Aguirre et al., 2016).

PLA has processing characteristics comparable to conventional thermoplastics (Armentano et al., 2013), and optical, thermal and mechanical properties similar to polypropylene (PP), poly(ethylene terephthalate) (PET), and polystyrene (PS) (Castro-Aguirre et al., 2016); nevertheless, it presents high brittleness, a rather low heat deflection temperature and high gas permeability, limiting its use for packaging purposes (Armentano et al., 2013; Murariu and Dubois, 2016). Many of PLA's limitations, especially mechanical ones such as excessive brittleness, low toughness and low impact resistance, have been minimized by the addition of plasticizers or flexible polymers (Pluta et al., 2006; Balakrishnan et al., 2010; Gunning et al., 2014), organic compounds such as ionic liquids (Chen et al., 2013), and (nano)fillers, as calcium carbonate (Jiang et al., 2007), silica (Kontou et al., 2011, 2012), zinc oxide (Huang et al., 2015), graphene (Bouakaz et al., 2015) and organoclays (Kontou et al., 2011; Fukushima et al., 2013; Pirani et al., 2013; Baouz et al., 2015).

We have previously published the study of the chemical composition effect of different Brazilian organic-modified montmorillonites (OMt) in PLA clay polymer nanocomposites (CPN), as well as the morphology and thermal properties (Alves et al., 2019), and thermal stability and fire performance as a function of the type of organoclay modifier (Alves et al., 2020). Organic-modified montmorillonites with low compatibility with PLA led to the formation of partially-intercalated nanocomposites and microcomposites, while those with good compatibility resulted in partially-intercalated/exfoliated nanocomposites. It was observed that the phosphonium-based montmorillonite was not well dispersed in PLA due to the low compatibility of this surfactant and PLA. On the other hand, hybrid organo-montmorillonite (HOMt) containing di(alkyl ester) dimethyl ammonium chloride (EA) and ethoxylated tallow amine (ETA) as second surfactant promoted better compatibility with PLA due to the presence of polar groups in their structure. The thermal degradation studies also revealed that the thermal stability of PLA nanocomposites was affected by the dispersion of organoclays and that the high amount of phosphonium-containing organoclays caused the

greatest reduction in the thermal stability of the materials due to thermal degradation of PLA chains (Alves et al., 2020).

Dynamic-mechanical-thermal analysis (DMTA) is a technique widely used to study the mechanical and viscoelastic behavior of polymeric materials as a function of temperature. From the DMTA data it is possible to determine the mechanical parameters related with viscoelasticity of the materials, such as the storage modulus (E'), related to the elastic response and stiffness of the material; the loss modulus (E"), related to the viscous response of the material; and the damping factor (tan δ), defined as the ratio between the former (tan δ = E"/E'), which quantifies the energy dissipation capacity of the material. In addition, it is also possible to verify primary (crystallization, melting), secondary (glass transition) and tertiary relaxation transitions. For polymer nanocomposites, one of the main objectives of this technique is to study the changes in these macroscopic properties with nano/microscopic conformational changes of the materials by the addition of nanofillers (Chartoff and Sircar, 2004; Menard and Menard, 2015).

Motivated by these previous works that reported a great innovation in the use of hybrid organoclays based on dual surfactants and the great potential of the PLA nanocomposites developed by these materials for high performance applications, the present work aims to evaluate the effect those different types of OMt on the mechanical and dynamic-mechanical-thermal and fracture mechanism of PLA/OMt nanocomposites, focusing on their developed structures and OMt-PLA interactions.

2. Materials and Methods

2.1. Materials

Single and hybrid organically-modified montmorillonites modified by a semi-solid method with different kinds of surfactants, namely di-(hydrogenated tallow) dimethyl ammonium chloride (HTA), trihexyl tetradecyl phosphonium chloride (TDP), di(alkyl ester) dimethyl ammonium chloride (EA) and ethoxylated tallow amine (ETA), were used to prepare nanocomposites based on a PLA (Ingeo 3052D) supplied by NatureWorks LLC with a D-lactide content around 4%. The materials and methods used to prepare the different organic-modified montmorillonites are described in previous works (Alves et al., 2016, 2017, 2018). For

comparison purposes, commercial organoclays Cloisite 20A and Cloisite 30B, supplied by Southern Clay Products, were used.

2.2. Samples preparation

A counter-rotating internal mixer (Brabender Plasti-Corder® W50EHT) was used to prepare PLA masterbatches with 20 wt% of organoclay, and a co-rotating twin screw extruder (Collin Kneter 25X36D), with diameter of 25 mm and L/D of 36 was used to dilute the masterbatches, producing clay PLA nanocomposites with 2 wt%, 6 wt% and 8 wt%. More details about the preparation method are given in a previous work (Alves et al., 2019). Virgin PLA was extruded at the same conditions and labeled as EPLA. A description of all material samples with their respective organoclay type(s) and content used to prepare the PLA nanocomposites is summarized in **Table 1**.

Table 1. Composition of PLA nanocomposites.

CPN code	Organoclay [(1)]	Organoclay content (wt%)	Surfactant type [(1)] and amount [(2)]
PN2MHTA	MHTA	2	HTA
PN6MHTA		6	
PN8MHTA		8	
PN2MTDP	MTDP	2	TDP
PN6MTDP		6	
PN8MTDP		8	
PN2HMPHTA	HMPHTA	2	14 wt% of TDP / 17 wt% of HTA
PN6HMPHTA		6	
PN8HMPHTA		8	
PN2HMPEA	HMPEA	2	12 wt% of TDP / 20 wt% of EA
PN6HMPEA		6	
PN8HMPEA		8	
PN2HMPETA	HMPETA	2	18 wt% of TDP / 9 wt% of ETA
PN6HMPETA		6	
PN8HMPETA		8	

PN2C30B		2	
PN6C30B	C30B	6	MT2EtOH
PN8C30B		8	
PN2C20A		2	
PN6C20A	C20A	6	HTA
PN8C20A		8	

(1) HTA: Dihydrogenated tallow dimethyl quaternary ammonium ion. TDP: Trihexyl tetradecyl quaternary phosphonium. EA: Dialkyl ester dimethyl quaternary ammonium ion. ETA: Ethoxylated tallow amine. MT2EtOH: Methyl tallow bis-2-hydroxyethyl quaternary ammonium ion.
(2) Surfactant amount determined by TGA (in nitrogen atmosphere).

2.3. Characterization procedure

Dynamic-mechanical-thermal analysis (DMTA) was carried out using a TA Instruments Q800 apparatus, in single cantilever mode, with a constant strain of 0.02% and frequency of 1 Hz, from 30 to 145 °C at 2 °C/min, using a minimum of two specimens with typical dimensions of 35.6 mm (length) × 12.7 mm (width) × 3.0 mm (thickness).

The flexural properties were determined by three-point bending according to standard ISO 178, using a Galdabini Sun 2500 equipment with a load cell of 5 kN. Tests were performed at room temperature using a minimum of four specimens per material, with typical dimensions of 60.0 mm (length) × 10.0 mm (width) × 3.0 mm (thickness), under a constant velocity of 5 mm/min.

The impact properties were determined by Charpy impact testing using a Zwick HIT 5.5P equipment according to standard ISO 179-1. The tests were carried out using a hammer with a maximum amount of energy of 1 J with perpendicular impact to the thinner face of both notched and un-notched specimens; a minimum of three specimens per material, with typical dimensions of 80.0 mm (length) × 10.0 mm (width) × 4.0 mm (thickness), were used. The notch was made with a radius of 0.25 mm and depth of 2.0 mm (type A).

Scanning Electron Microscopy (SEM) was used to study the morphology and the fracture behavior of the fractured surfaces of three-point bending and impact specimens. The images were obtained using a JEOL JSM-5610 microscope applying a voltage of 15 kV and a

working distance of 30 mm. The samples were prepared at room temperature by depositing a thin layer of gold on the fractured surface using a BAL-TEC SCD005 sputter coater (argon atmosphere).

3. Results and discussion

3.1. Dynamic-mechanical-thermal properties

Characteristic curves of the evolution of the storage modulus (E'), loss modulus (E") and tan δ with temperature are shown in **Figure 1**. CPN materials displayed T_g values slightly lower than EPLA. The increase in T_g observed in E' curves and the decrease in tan δ curves above 95 °C are associated to the cold crystallization of PLA. The results summarized in **Table 2** feature a gradual decrease in the onset of cold crystallization temperature ($T_{cc.onset}$) of PLA by the addition of all OMt. These results were similar to the ones determined by the first heating in DSC results (Alves et al., 2019).

Analyzing the glassy plateau (E' at 30°C in **Figure 1** and in **Table 2**), it can be seen that the storage modulus of most of the materials was slightly enhanced by increasing OMt content. The enhancement was more pronounced in nanocomposites containing C30B, C20A, MHTA and HMPEA. The increment in E' with OMt content is associated with the reinforcing effect offered by the dispersed rigid-structures (Krikorian and Pochan, 2003; Sinha Ray et al., 2003; Kontou et al., 2011). The enhancement effect depends on the dispersion degree of the nanostructures, as well as the interfacial interaction between the phases (Sinha Ray et al., 2003; Kontou et al., 2011). Therefore, these results are in agreement with structural and morphological analyses presented in previous work (Alves et al., 2019), justifying the higher storage modulus of PLA nanocomposites with C30B.

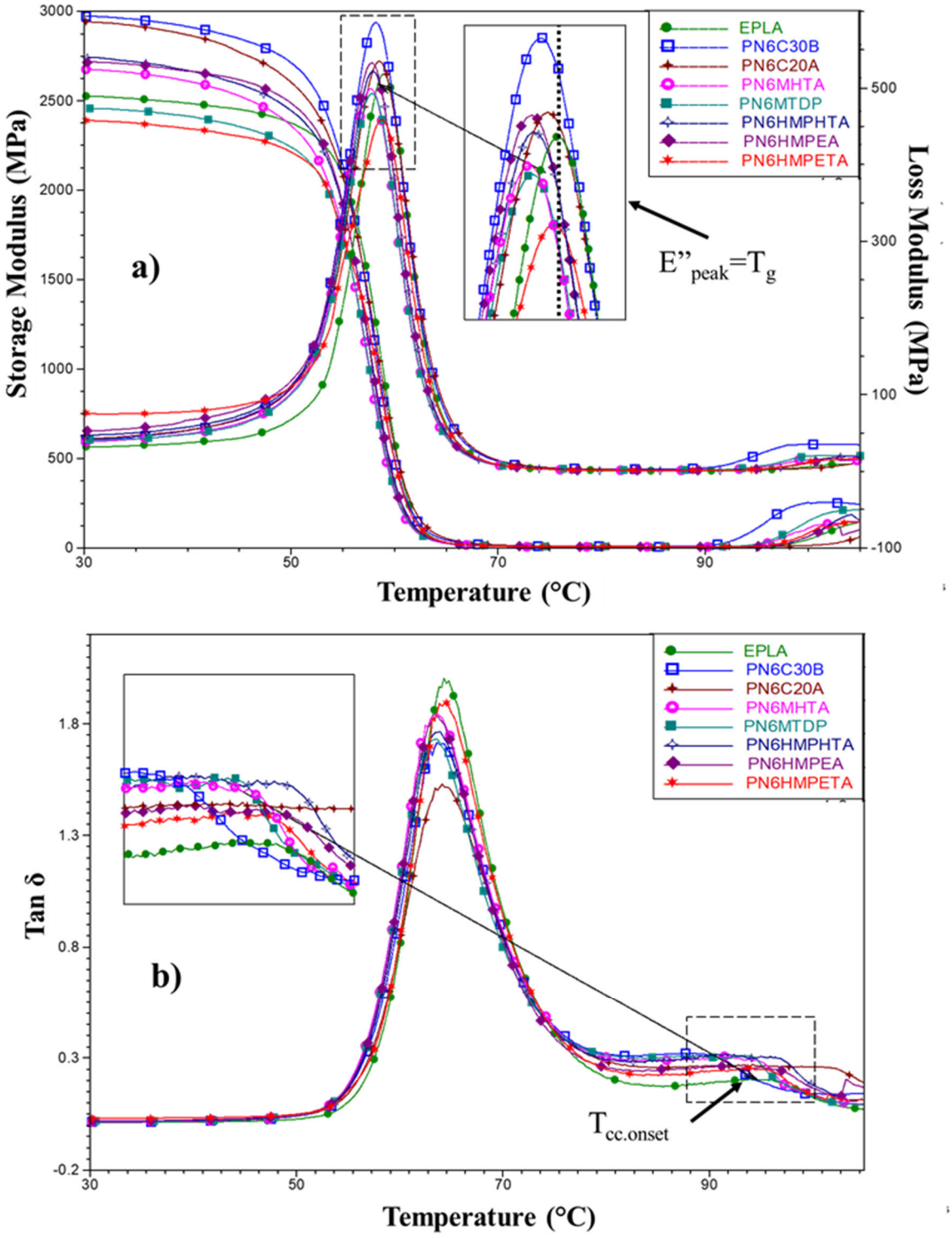

Figure 1. Representative curves of the evolution of the (a) storage modulus (E') and loss modulus (E''), and (b) tan δ with temperature for PLA and CPN with 6 wt% of OMt.

Table 2. Glass transition temperature (T_g), onset of cold crystallization temperature ($T_{cc.onset}$) and storage modulus of PLA nanocomposites.

CPN code	T_g (°C) (1)	$T_{cc.onset}$ (°C) (2)	E' (MPa) (3)

PLA	60	97	2562
PN2MHTA	58	96	2673
PN6MHTA	58	95	2738
PN8MHTA	58	93	2812
PN2MTDP	59	94	2588
PN6MTDP	58	94	2500
PN8MTDP	57	91	2639
PN2HMPHTA	58	96	2536
PN6HMPHTA	58	96	2771
PN8HMPHTA	58	94	2783
PN2HMPEA	58	93	2674
PN6HMPEA	58	95	2733
PN8HMPEA	58	97	2798
PN2HMPETA	59	92	2575
PN6HMPETA	59	95	2510
PN8HMPETA	59	94	2561
PN2C30B	59	90	2626
PN6C30B	58	91	3112
PN8C30B	57	91	3298
PN2C20A	59	96	2599
PN6C20A	59	102	2921
PN8C20A	58	100	3027

(1) T_g determined at the maximum of the loss modulus curve.
(2) $T_{cc.onset}$ determined at the second peak of the tan δ curve.
(3) Storage modulus determined at 30 ºC.

PLA nanocomposites prepared with MTDP and HMPETA caused nearly no change in E', which can be associated to the reduction of molecular mass by thermal degradation during extrusion, as suggested by TGA and GPC discussion in previous work (Alves et al., 2020). Furthermore, it was reported that at high OMt content the chain confinement effect can be reduced and there is a reduction of the fillers/matrix contact area due to an increase in the number of OMt agglomerates (Kontou et al., 2011, 2012; Pirani et al., 2013). Indeed, the increase of C30B content from 2 wt% to 6 wt% caused a significant increase in E' for PNC30B nanocomposites, but the same was not observed for 8 wt%.

3.2. Flexural properties

PLA is well known for its excessive brittleness. The improvement of the toughness of PLA without loss of other properties, such as elastic modulus or thermal stability, has been the

aim of several studies (Jiang et al., 2007; K. et al., 2012; Baouz et al., 2015; Nur-Aimi and Anuar, 2016). Flexural and impact tests were performed on EPLA and PLA nanocomposites aiming to evaluate the influence of OMt's type and content on the mechanical performance of PLA nanocomposites.

The flexural stress-strain curves of PLA nanocomposites are presented in **Figure 2**, the variation of the flexural modulus and strength in **Figure 3**, and the variation of the flexural strain and toughness in **Figure 4**. The flexural modulus and flexural strength of PLA nanocomposites exhibited a contrary trend regarding OMt's content. Overall, the flexural modulus slightly increased by the addition of all OMt, and by increasing their concentration, whereas the flexural strength gradually decreased.

Generally speaking, the flexural modulus of PLA nanocomposites displayed a similar trend as the storage modulus presented in the prior section. The enhancement of the flexural modulus observed for the nanocomposites when compared with EPLA is due to the reinforcement effect of the dispersed nanoclay structures in the matrix, acting as rigid fillers absorbing and supporting the external mechanical load. This enhancement was less pronounced when using MTDP and the three HOMts – MPHTA, MPEA and MPETA, which can be associated with molar mass reduction, as reported in a previous work (Alves et al., 2020), probably due to the high phosphonium salt content in these materials, which showed to be quite incompatible with PLA matrix (Alves et al., 2019, 2020). The increase of the modulus with augmenting OMt content may be associated to the presence of small clay stacks/agglomerates well distributed throughout the matrix that can influence the stiffness more than exfoliated structures (Lai et al., 2014). The occurrence of those microstructures (agglomerates of clay stacks) was observed in TEM micrographs and shown in a previous work (Alves et al., 2019). They do not provide sufficient interfacial interactions/adhesion between the phases, which can lead to an easy debonding of these particles from the matrix at lower stress, even lower than the yield point of the matrix. Such structures acted as defects and stress concentrators, creating localized weakening points that reduced the material strength (LAI et al., 2014), supporting the the evolution of the flexural strength with OMt's content.

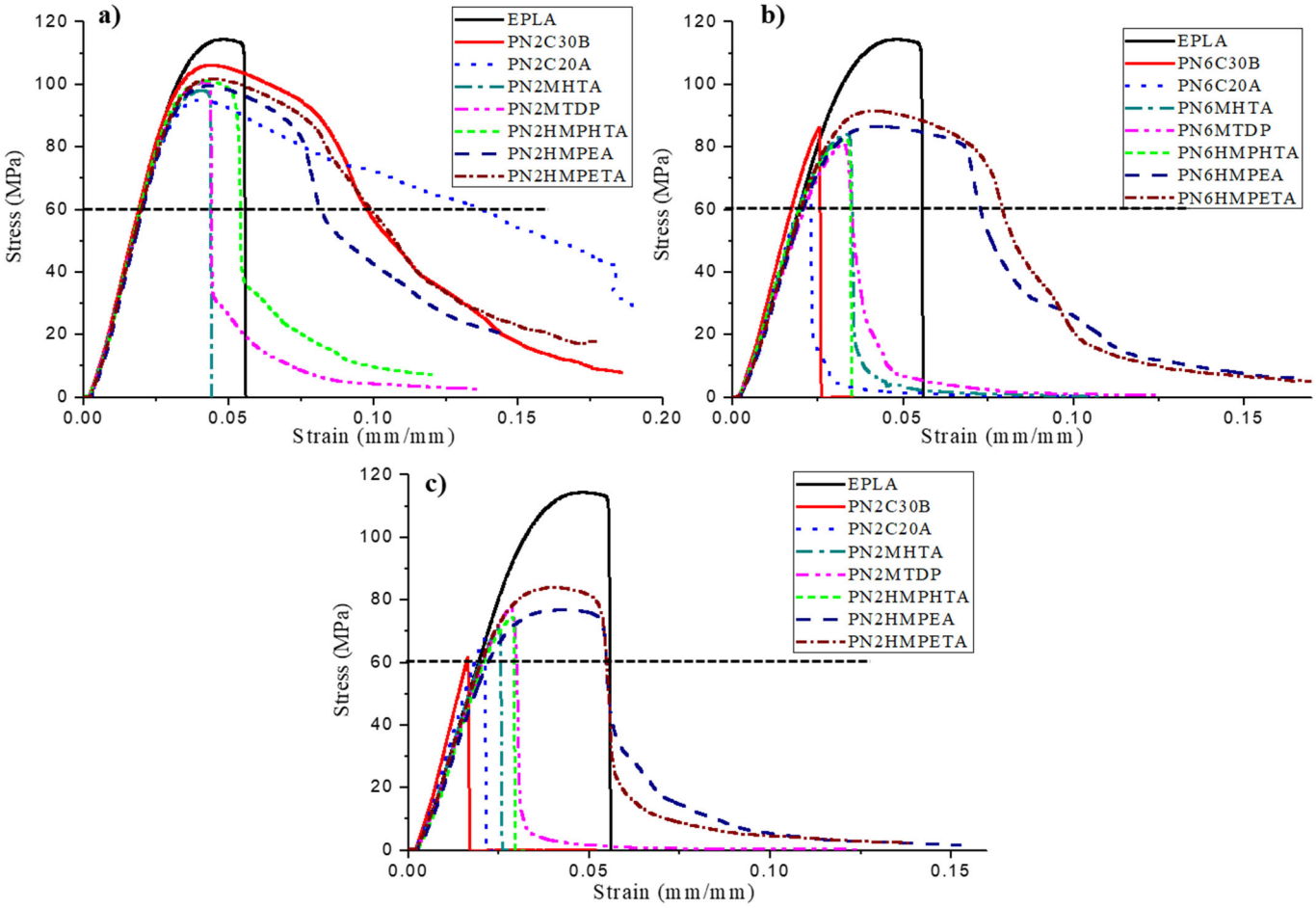

Figure 2. Flexural stress-strain curves of PLA nanocomposites with (a) 2 wt%, (b) 6 wt% and (c) 8 wt% of OMt.

The flexural strain at break was not easy to determine as can be seen in **Figure 2**, as in some cases the material did not break or it was difficult to identify in the curve. Thus, to evaluate the elongation behavior of the materials, the maximum flexural strain was determined at the stress drop at 60 MPa (indicated in **Figure 2**). The flexural strain and toughness, determined as the area below the stress-strain curve, are presented in **Figure 4**. In general, both properties followed the same trend. EPLA displayed a typical brittle-like mechanical behavior, breaking with nearly no plastic deformation at 5.5% of strain with a toughness of 4.5 MJ/m^3. The addition of most of the organoclays, mainly at high content, increased the brittleness of PLA, as can be seen by the flexural strain and toughness results.

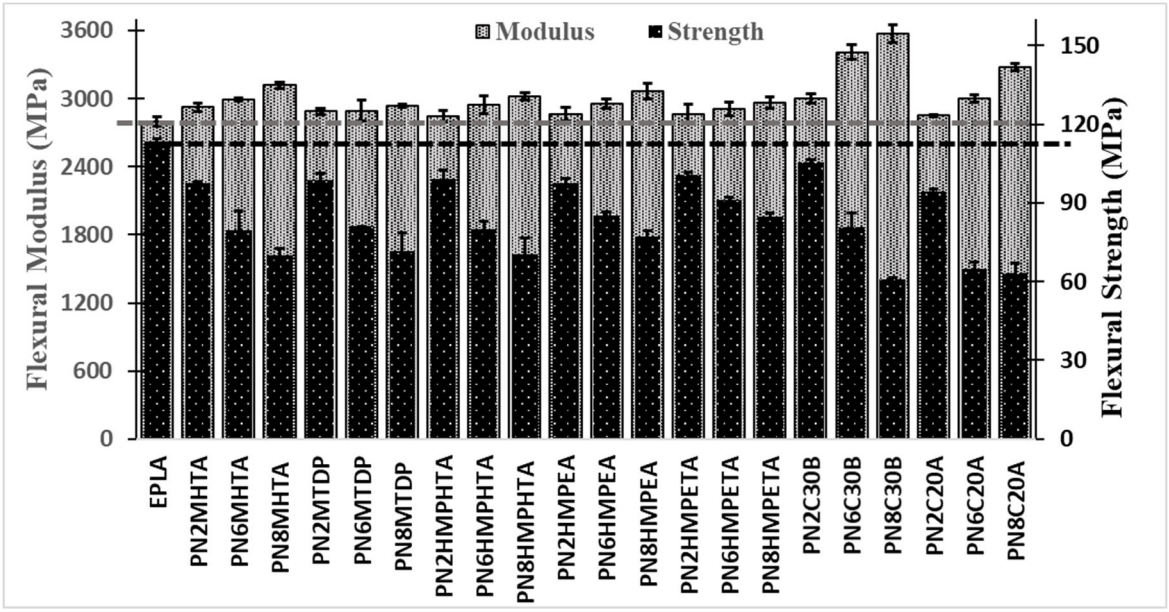

Figure 3. Evaluation of the flexural modulus and flexural strength with OMt type and content. Dotted lines indicate the values of EPLA.

The ductility of PLA was significantly enhanced by adding 2 wt% of MPEA, MPETA, C30B and C20A, which led to an increase in the flexural strain of around 10% and in the toughness of around 8 MJ/m^3. However, looking to the CPN series with C30B and C20A (**Figure 4**), when the OMt content raised to 6 wt% and 8 wt%, both the flexural strain and the toughness drastically dropped to values lower than those of EPLA. These materials fractured in a completely brittle manner without yielding **(Figure 2**). Lai et al. (2014) reported a large elongation at break under tensile testing of more than 200% in PLA nanocomposites with only 1 phr of C30B, which drastically decreased to values lower than that of PLA by increasing OMt's content to 3 and 5 phr. This same trend was also found by Acik et al. (2016), which observed an enhancement of the tensile elongation of PLA/C30B nanocomposites with 1 wt% to 3 wt% of organoclays and a drastic drop after 4 wt%. In contrast with these studies, this work shows that the content increase of the two hybrid OMts, HMPEA and HMPETA, caused a lighter reduction of these properties when compared to other organoclays. For a content of 6 wt% the flexural strain was higher than PLA's at around 7.0% and 9.5%, and toughness was 5 MJ/m^3 and 6.2 MJ/m^3, respectively for MPEA and MPETA. This can be associated to a plasticizing effect caused by the good dispersion and good interfacial interaction of these organoclays with PLA provided by the EA and ETA surfactants used in these hybrid OMts, improving toughness. For a content of 8 wt% of these organoclays, the strain was almost the same as PLA's and the toughness was slightly reduced. Besides, plastic deformation can still be observed in the curves of these nanocomposites (see **Figure 2c**).

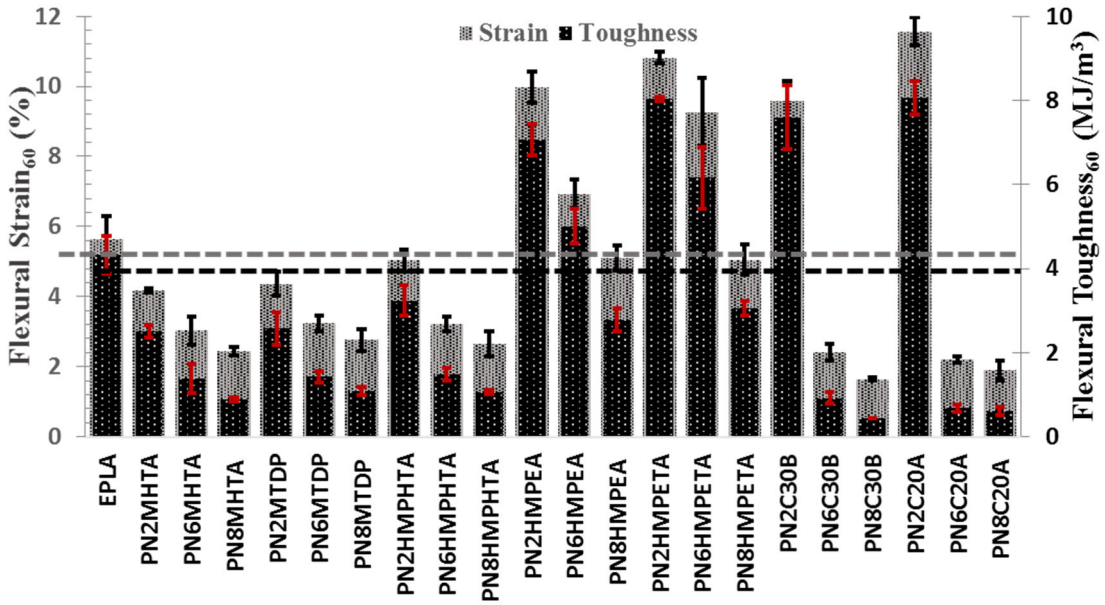

Figure 4. Evaluation of the flexural strain and flexural toughness at a stress of 60 MPa with OMt type and content. Dotted lines indicate the values of EPLA.

3.3. Impact properties

The results of the impact resistance are shown in **Figure 5**. Nearly no improvement in un-notched and notched impact resistance was achieved by adding most of the organoclays, in some cases the impact resistance decreasing with augmenting OMt's content.

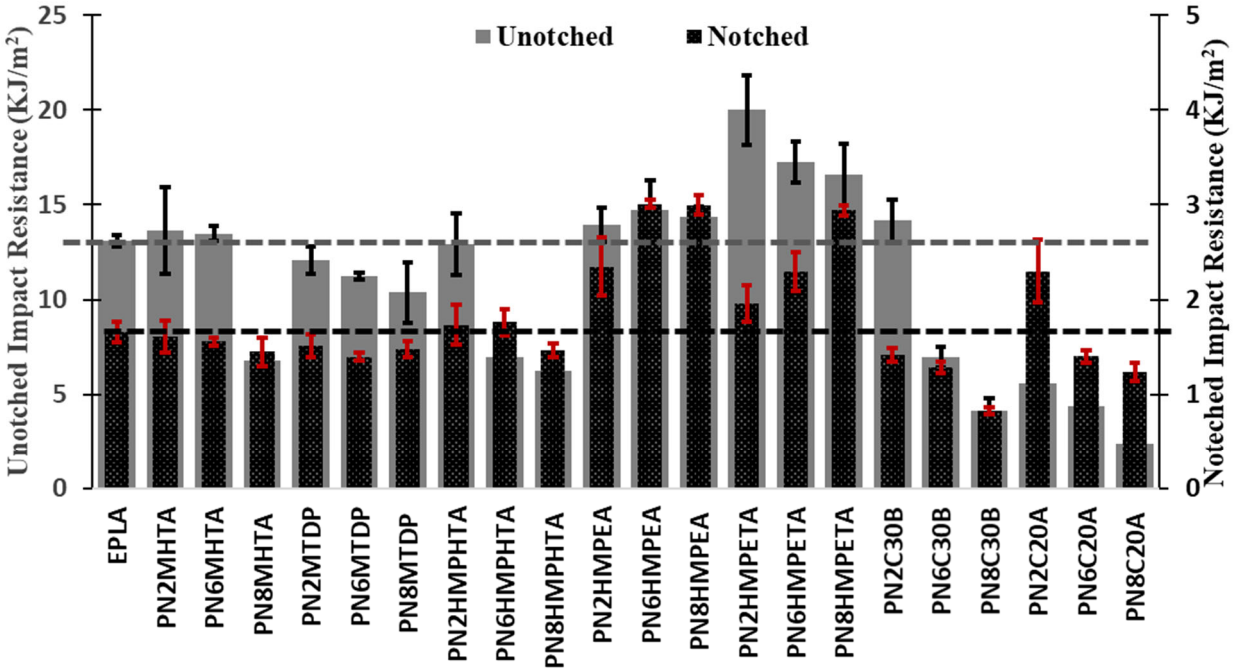

Figure 5. Evaluation of the impact resistance with organic-modified montmorillonites (OMt) type and content. Dotted lines mark the values of EPLA.

A great enhancement, comparing with EPLA, was achieved for PLA nanocomposites with HMPEA and HMPETA. The un-notched impact resistance of these materials slightly decreased with OMt's content, whereas the notched ones surprisingly improved with OMt's content. This mechanical property strongly depends on the dispersion degree of nanoparticles as well as the interfacial interaction between phases. The gradual decrease of the un-notched impact resistance can be explained by the large microstructures formed by increasing the amount of OMt, which acted as local stress concentrators that favored the initial crack formation by debonding/cavitation of these microparticles at lower critical stress/energy. On the other hand, crack propagation depends on the adhesion and dispersion degree of the micro and nanostructures in the matrix. Thus, in the case of notched specimens, the notch acted as initial crack, which means that enhancement in the impact resistance was associated to a good dispersion and interfacial interaction between HMPEA/HMPETA and PLA, which allowed an effective stress transfer from the matrix to the fillers and a barrier effect that limited crack propagation. Therefore, PLA nanocomposites with HMPEA/HMPETA had their toughness and impact resistance enhanced due to the good dispersion of the nanoparticles and strong interaction with PLA, as suggested by Alves et al. (2019).

Albeit PN2C20A nanocomposites presented a notched impact resistance higher than that of EPLA, it substantially decreased with augmenting OMt's content to values lower than EPLA. Surprisingly, blending PLA with 2 wt% of C30B caused nearly no enhancement in the impact resistance and drastically decreased with further increasing OMt's content. It was expected that this property, alongside flexural toughness, would increase with at least 2 wt% of C30B due to the good dispersion of C30B and good interaction between PLA and C30B.

3.4. Toughening mechanism and morphology of the fracture surface

Flexural and impact results provided information that the dispersion of the different types of organoclay affected the mechanical behavior of PLA. Even at high content, HMPEA and HMPETA caused a transition on PLA deformation behavior from mainly brittle or quasi-brittle to ductile. The mechanisms of energy absorption in brittle polymers has been widely

discussed in the literature and strongly associated to catastrophic crack propagation and crazing (Park et al., 2006; Jiang et al., 2007; Stoclet et al., 2014; Baouz et al., 2015; Nur-Aimi and Anuar, 2016). Crazing is a localized cavitational mechanism characterized by the formation of interpenetrating microvoids bridged by polymer fibrils (fine filaments formed by molecules of the stretched backbone polymer chains) in a region of the material under high localized tensile stress and/or yielding. Fibrils act as anchors hindering crack spread and, depending on the applied tensile stress, microvoids growth and coalesced forming cracks until the material ruptures (Stoclet et al., 2014; Nur-Aimi and Anuar, 2016).

Macroscopic stress whitening zone in the zone under tensile loading (opposite side of load application) was reveled in the flexural specimens of some nanocomposites, mainly the ones that presented plastic deformation behavior observed in **Figure 2**. Such characteristics can be seen in **Figure 6**.

EPLA's specimen ruptured in a brittle manner into two portions with no sign of plastic deformation. On the other hand, all nanocomposite specimens with HMPEA and HMPETA displayed a whitening region, typically associated to a crazing mechanism, and did not completely break into two portions until the maximum elongation used in the tests of around 20%. To reach such accomplishments, a high extent of well-dispersed nanofillers with high aspect ratio is necessary, besides a high compatibility between polymer and clay modifier, in order to allow interfacial interaction (Jiang et al., 2007; Baouz et al., 2015; Nur-Aimi and Anuar, 2016). This explanation supports the morphology and the change in fracture behavior by blending PLA with the hybrid HMPEA and HMPETA organoclays, even at high concentration.

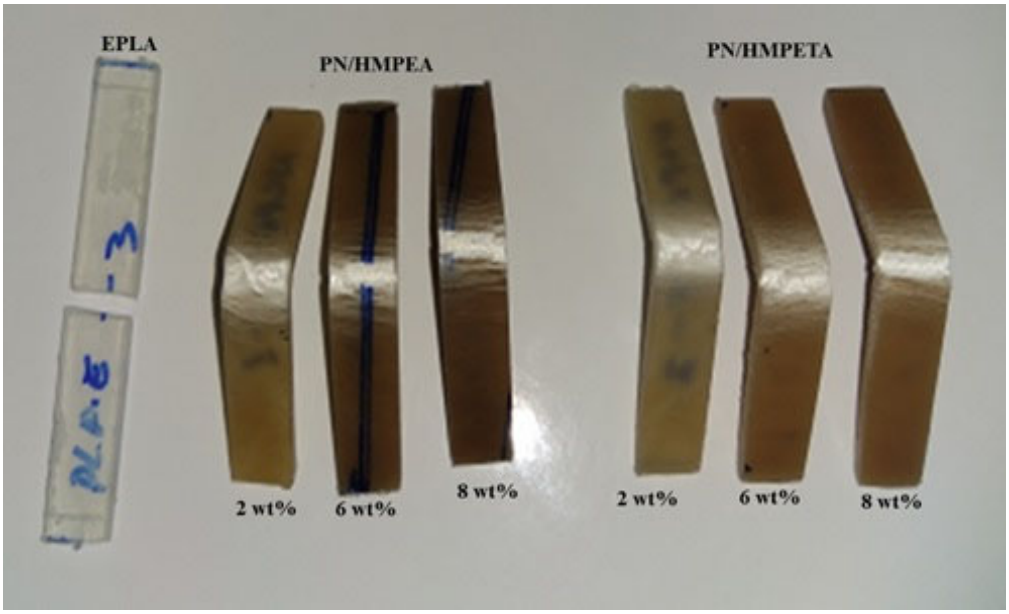

Figure 6. Specimens of EPLA and PLA nanocomposites with HMPEA and HMPETA after flexural testing showing whitening of the crazed region.

The fracture surface of some flexural specimens studied by SEM can be seen in **Figure 7** and in **Figure 8**. The SEM micrograph of EPLA shows a smooth surface with nearly no sign of plastic deformation, which confirmed that PLA sample broke quickly due to fast development and propagation of critical cracks. PLA nanocomposites with 2 and 8 wt% of MTDP, which also featured nearly no yielding during flexural stress, exhibited a slight rough surface without microvoiding and almost no plastic deformation (**Figure 7b** and **Figure 7c**). A large amount of flaws from cavitation and debonding due to OMt agglomerates can be seen in the fracture surface, which confirmed the poor adhesion and low ductility promoted by this organoclay. On the other hand, the samples that displayed large yielding and intense stress whitening, as PN2C30B (**Figure 7d** and **Figure 7e**), PN2HMPEA (**Figure 8a** and **Figure 8b**) and PN2HMPETA (**Figure 8d** and **Figure 8e**), showed extensive plastic deformation (micrographs at low magnification). It happened due to a large amount of small microvoids surrounded by extensively oriented ligaments. That may be fibrils that were drawn out from the polymer under flexural stress, as can be seen in the micrographs at high magnification. It features that a lot of energy was absorbed before failure of these materials since these kind of mechanisms are associated to extensive local plastic deformation that leads to a larger strain-at-break and higher toughness.

Flexural curves suggested that the strength and toughness of PLA was negatively affected when the concentration of OMt increased, and the reason for that can be elucidated by

SEM micrographs of PLA nanocomposites with 8 wt% as presented in **Figure 7f**, **Figure 8c** and **Figure 8f**. The fracture surface of PN8C30B shows large voids/flaws associated with tactoids/agglomerates of clay particles and sign of waves from crack propagation. This suggests that the catastrophic failure of the material was caused by debonding of these microstructures that acted as stress concentrators, resulting in early critical crack formation and quick propagation. OMt clusters and cavities associated with microparticles debonding could also be seen by analyzing the fracture surface of nanocomposites with 8 wt% of HMPEA and HMPETA. However, these materials presented greater plastic deformation and no clear waves of crack propagation when compared to the samples with C30B. Indeed, these microsize structures led to the early fracture of the material with less energy than the ones with 2 wt%, but the good interaction of these organoclays still promoted microvoiding and shear band (plastic deformation), resulting in a more ductile material.

More information about the fracture toughening mechanisms could be obtained by analyzing the fracture surface of notched impact specimens, as presented in **Figure 9** and **Figure 10**. For EPLA (**Figure 9**) clear waves in the notch direction were found. This surface was characterized by a smooth surface with stress whitening due to fast matrix detachment, resulting in polymer fibrillation without microvoiding, as seen in the high magnification micrograph. Such morphology suggests that EPLA suffered an abrupt rupture under impact stress due to fast crack propagation with very low energy values.

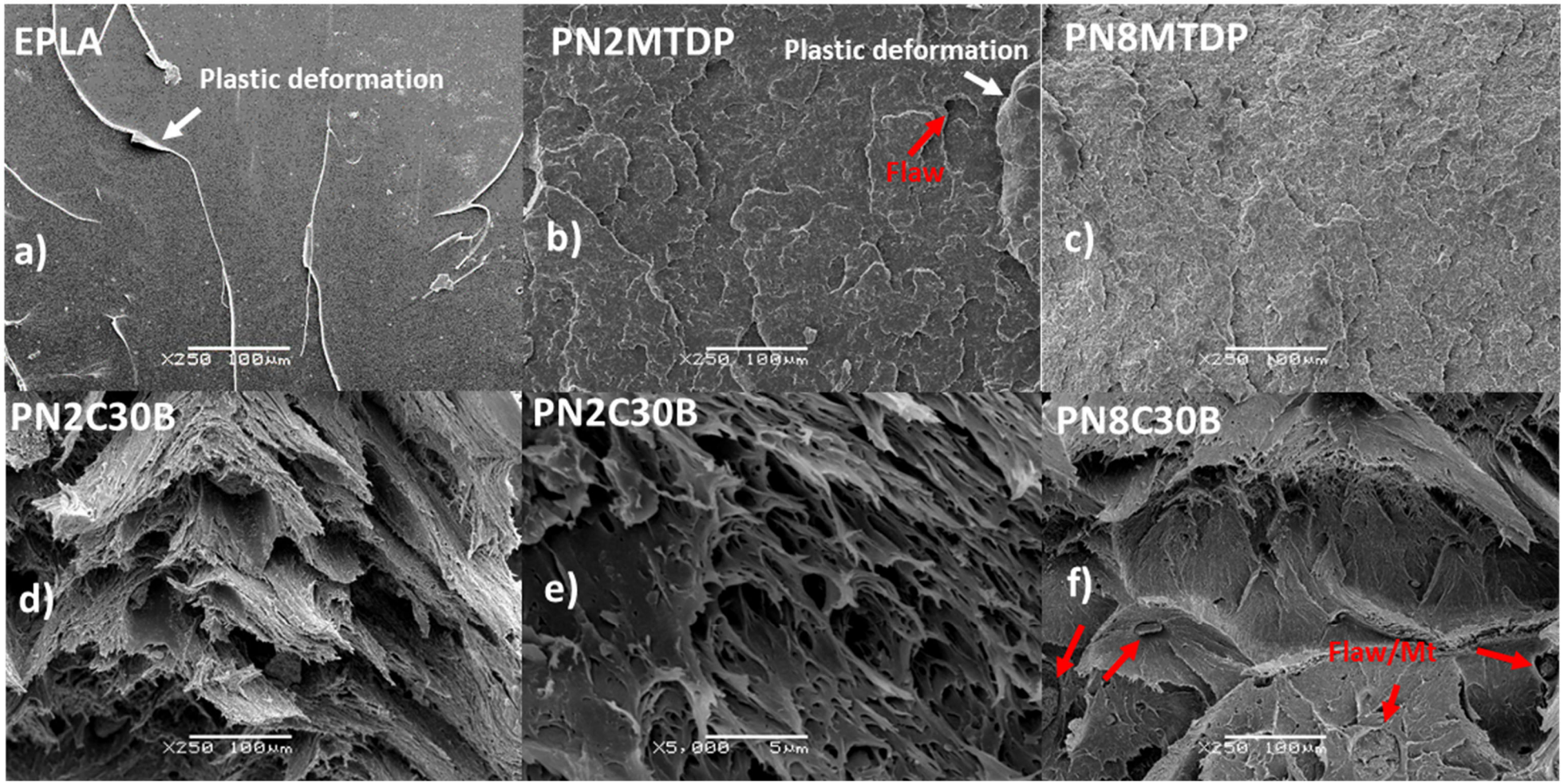

Figure 7. SEM micrographs of the fracture surfaces of flexural specimens: (a) EPLA, (b) PN2MTDP, (c) PN8MTDP, (d) PN2C30B at low magnification, (e) PN2C30B at high magnification and (f) PN8C30B.

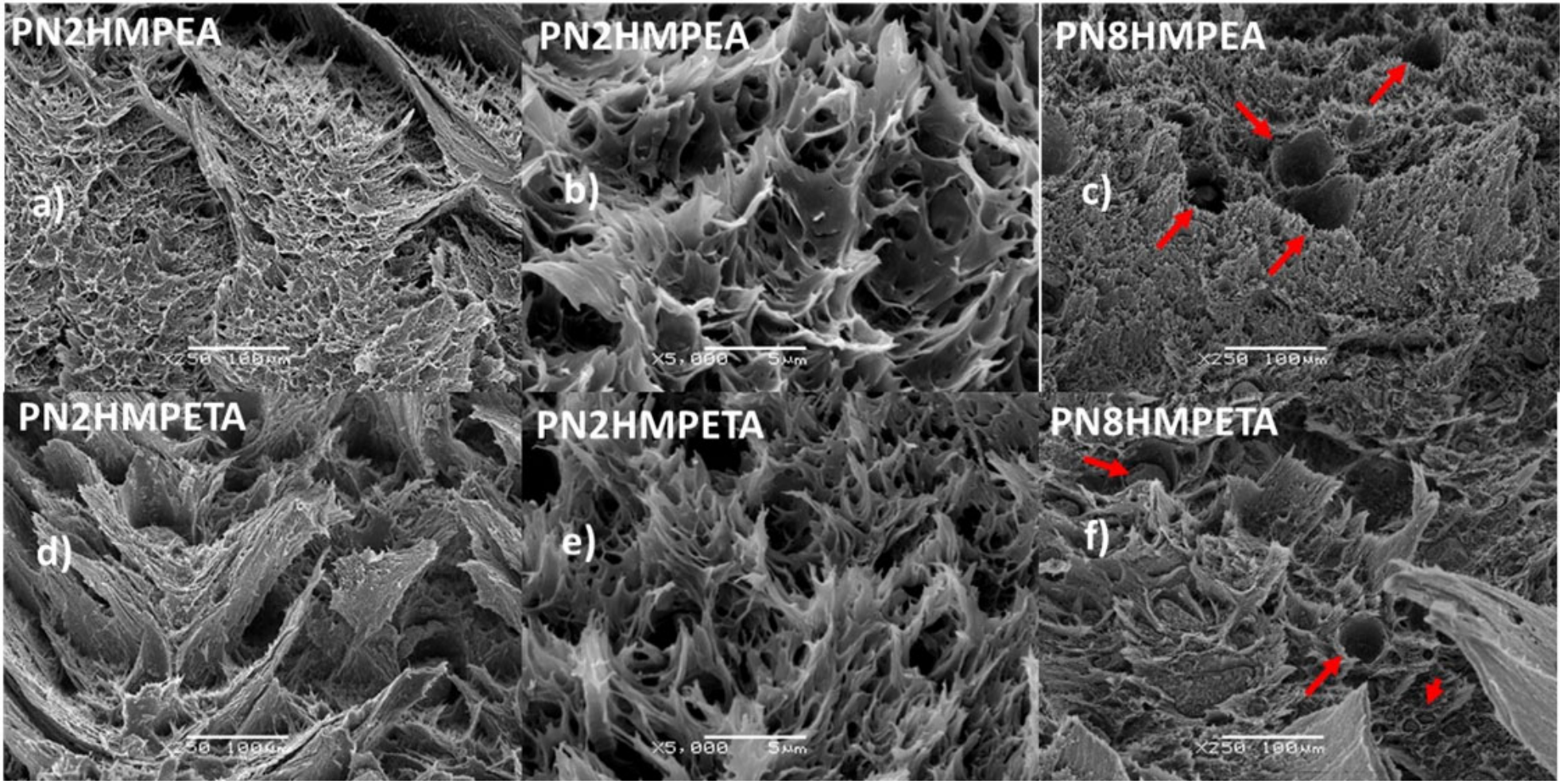

Figure 8. SEM micrographs of the fracture surfaces of flexural specimens: (a) PN2HMPEA at low magnification, (b) PN2HMPEA at high magnification, (c) PN8HMPEA, (d) PN2HMPETA at low magnification, (e) PN2HMPETA at high magnification and (f) PN8HMPETA.

As well as in flexural specimens, the impact fracture of PLA nanocomposites with HMPEA and HMPETA (**Figure 10**) exhibited a rougher surface than EPLA. The roughness on the fracture surface of both materials increased with augmenting OMt's content. The high magnification micrographs revealed an increasing in extent of microvoids and plastic deformation (fibrils) with OMt content. This behavior indicates that crazing and shear yielding mechanisms increased with HMPEA and HMPETA concentration. It was probably induced by the higher amount of well-dispersed and adhered stacks and platelets of OMt, which led to the enhancement of the material toughness under impact load as exhibited in **Figure 5**. Indeed, some OMt stacks can be seen well anchored to the matrix and embedded within the PLA matrix enveloped by microvoids on the fracture surface of PLA nanocomposites with 2 and 8 wt% of HMPEA (**Figure 10a'** and **Figure 10b'**). Thus, high energy was necessary to create these surfaces and to fracture these materials, which resulted in the enhancement of fracture toughness under impact test.

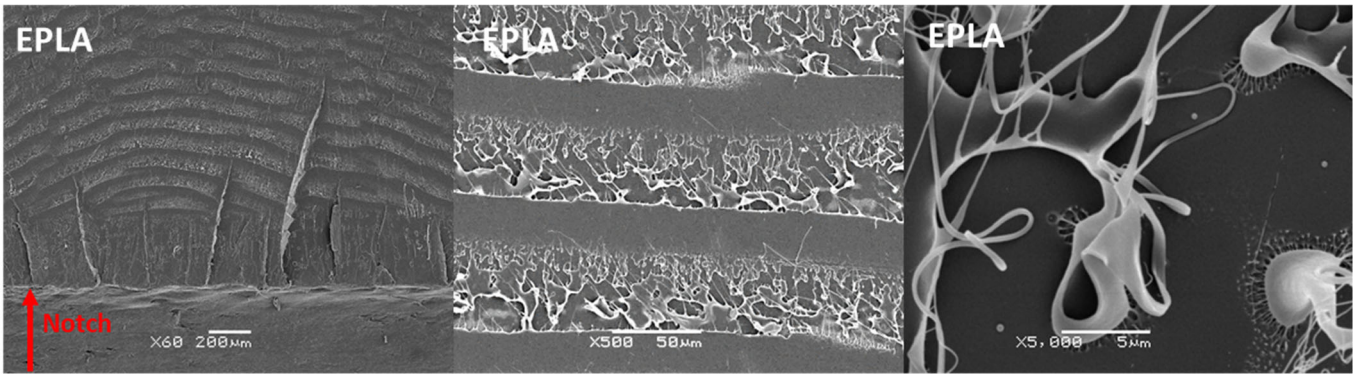

Figure 9. SEM micrographs of the fracture surfaces of notched impact specimens of EPLA at low, medium and high magnification.

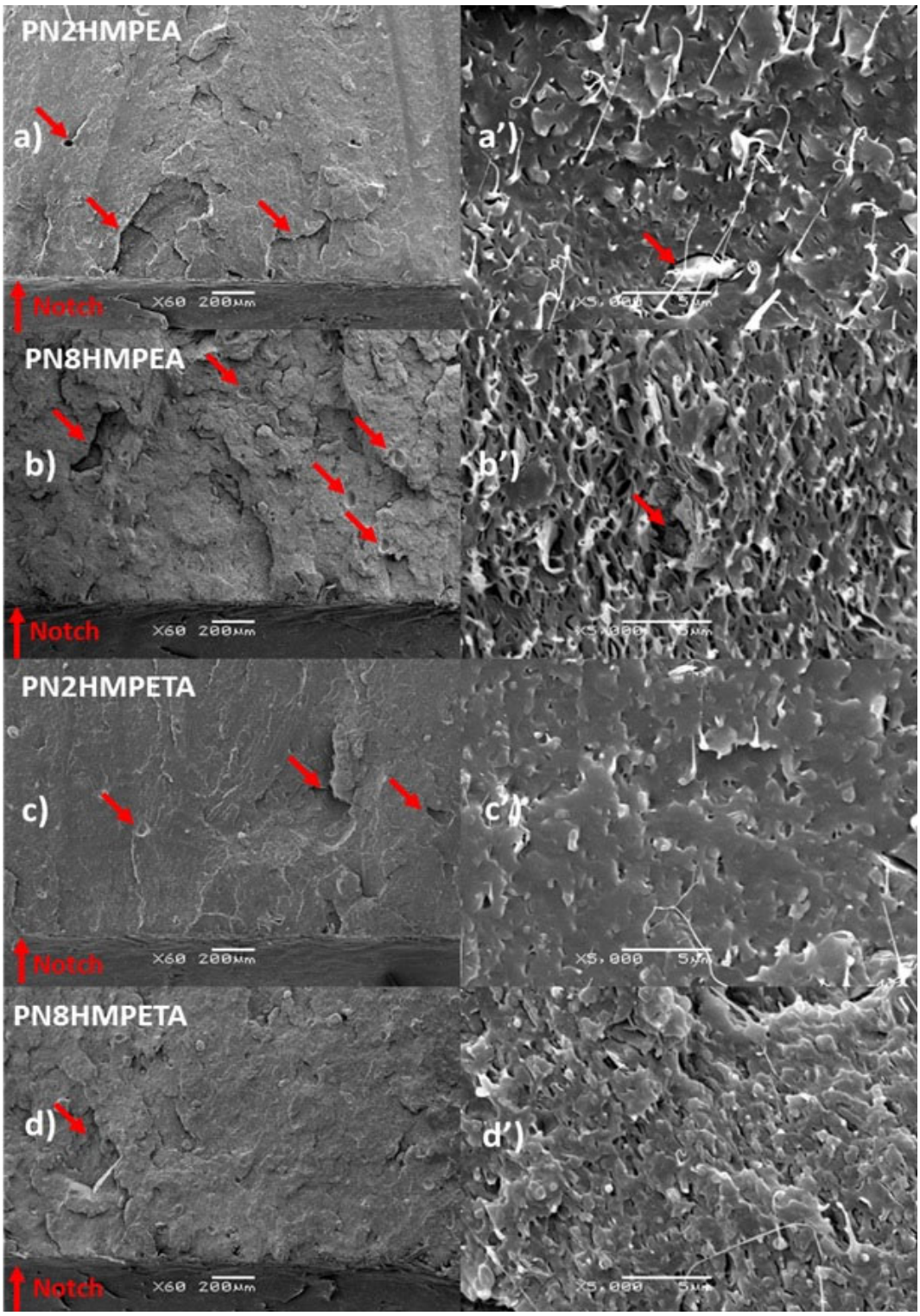

Figure 10. SEM micrographs of the fracture surfaces of notched impact specimens: (a) low and high magnification PN2HMPEA, (b) low and high magnification PN8HMPEA, (c) low and high magnification PN2HMPETA and (d) low and high magnification PN8HMPETA.

The fracture behavior of PLA was in fact influenced by OMt's chemical composition and concentration. The toughness of PLA, as suggested by flexural and impact tests, was mainly increased

when adding HMPEA and HMPETA due to its good dispersion and interfacial interaction. Such morphology created physical barriers to the coalescence of crazes and crack propagation, diverting it in random directions. In addition, the partially-exfoliated nanostructure, coupled with the PLA by strong interactions, allowed an effective matrix toughness increase by crazing and multi-shear banding mechanisms, induced by a highly plasticized interfacial region around the nanoclays (Lai et al., 2014).

4. Conclusions

The effect of organic-modified montmorillonites chemical composition on the morphological, thermal and mechanical properties of PLA nanocomposites was studied. DMTA, flexural and impact testing provided evidences that the degree of compatibility between the clay modifiers and PLA governs the morphology of PLA nanocomposites and consequently affects their mechanical properties.

The hybrid organo-montmorillonites containing ester ammonium (EA) and ethoxylated amine (ETA) promoted a high level of compatibility and interaction with PLA due to polar groups in their structures, enhancing the ductility and impact resistance of PLA nanocomposites. The toughening mechanism of PLA nanocomposites containing these organoclays was enhanced due to its good dispersion and strong interfacial interactions between the phases, which promoted localized plastic deformation induced by crazing and shear band mechanisms.

Acknowledgments

The authors acknowledge the Brazilian National Council of Scientific and Technological Development (CNPQ) [grant numbers: 142448/2013-3, 232751/2014-5] and the Spanish Ministry of Science and Innovation for the financial support of project MAT2017-89787-P.

References

Acik, E., Orbey, N., Yilmazer, U., 2016. Rheological properties of poly(lactic acid) based nanocomposites: Effects of different organoclay modifiers and compatibilizers. J. Appl. Polym. Sci. 133, 42915. https://doi.org/10.1002/app.42915

Ahmed, J., Varshney, S.K., 2011. Polylactides—Chemistry, Properties and Green Packaging Technology: A Review. Int. J. Food Prop. 14, 37–58. https://doi.org/10.1080/10942910903125284

Alves, J.L., Rosa, P. de T.V. e., Realinho, V., Antunes, M., Velasco, J.I., Morales, A.R., 2020. The effect of Brazilian organic-modified montmorillonites on the thermal stability and fire performance of organoclay-filled PLA nanocomposites. Appl. Clay Sci. 194, 105697.

https://doi.org/10.1016/j.clay.2020.105697
Alves, J.L., Rosa, P. de T.V. e., Realinho, V., Antunes, M., Velasco, J.I., Morales, A.R., 2019. Influence of chemical composition of Brazilian organoclays on the morphological, structural and thermal properties of PLA-organoclay nanocomposites. Appl. Clay Sci. 180, 105186. https://doi.org/10.1016/j.clay.2019.105186
Alves, J.L., Rosa, P. de T.V. e, Morales, A.R., 2018. Hybrid organo-montmorillonite produced by simultaneous intercalation of phosphonium and ammonium/amine based surfactants. Mater. Chem. Phys. 218, 279–288. https://doi.org/10.1016/j.matchemphys.2018.07.040
Alves, J.L., Rosa, P. de T.V. e, Morales, A.R., 2017. Evaluation of organic modification of montmorillonite with ionic and nonionic surfactants. Appl. Clay Sci. 150, 23–33. https://doi.org/10.1016/j.clay.2017.09.001
Alves, J.L., Rosa, P.D.T.V.E., Morales, A.R., 2016. A comparative study of different routes for the modification of montmorillonite with ammonium and phosphonium salts. Appl. Clay Sci. 132–133, 475–484. https://doi.org/10.1016/j.clay.2016.07.018
Armentano, I., Bitinis, N., Fortunati, E., Mattioli, S., Rescignano, N., Verdejo, R., Lopez-Manchado, M. a., Kenny, J.M., 2013. Multifunctional nanostructured PLA materials for packaging and tissue engineering. Prog. Polym. Sci. 38, 1720–1747. https://doi.org/10.1016/j.progpolymsci.2013.05.010
Balakrishnan, H., Hassan, A., Wahit, M.U., Yussuf, A.A., Razak, S.B.A., 2010. Novel toughened polylactic acid nanocomposite: Mechanical, thermal and morphological properties. Mater. Des. 31, 3289–3298. https://doi.org/10.1016/j.matdes.2010.02.008
Baouz, T., Acik, E., Rezgui, F., Yilmazer, U., 2015. Effects of mixing protocols on impact modified poly(lactic acid) layered silicate nanocomposites. J. Appl. Polym. Sci. 132, 1–14. https://doi.org/10.1002/app.41518
Bouakaz, B.S., Pillin, I., Habi, A., Grohens, Y., 2015. Synergy between fillers in organomontmorillonite/graphene-PLA nanocomposites. Appl. Clay Sci. 116–117, 69–77. https://doi.org/10.1016/j.clay.2015.08.017
Castro-Aguirre, E., Iñiguez-Franco, F., Samsudin, H., Fang, X., Auras, R., 2016. Poly(lactic acid)—Mass production, processing, industrial applications, and end of life. Adv. Drug Deliv. Rev. https://doi.org/10.1016/j.addr.2016.03.010
Chen, B.-K., Wu, T.-Y., Chang, Y.-M., Chen, A.F., 2013. Ductile polylactic acid prepared with ionic liquids. Chem. Eng. J. 215–216, 886–893. https://doi.org/10.1016/j.cej.2012.11.078
Fukushima, K., Tabuani, D., Arena, M., Gennari, M., Camino, G., 2013. Effect of clay type and loading on thermal, mechanical properties and biodegradation of poly(lactic acid) nanocomposites. React. Funct. Polym. 73. https://doi.org/10.1016/j.reactfunctpolym.2013.01.003
Garlotta, D., 2001. A Literature Review of Poly(Lactic Acid). J. Polym. Environ. 9, 63–84.

https://doi.org/10.1023/A:1020200822435
Gunning, M.A., Geever, L.M., Killion, J.A., Lyons, J.G., Chen, B., Higginbotham, C.L., 2014. The effect of the mixing routes of biodegradable polylactic acid and polyhydroxybutyrate nanocomposites and compatibilised nanocomposites. J. Thermoplast. Compos. Mater. 1–20. https://doi.org/10.1177/0892705714526912
Huang, Y., Wang, T., Zhao, X., Wang, X., Zhou, L., Yang, Y., Liao, F., Ju, Y., 2015. Poly(lactic acid)/graphene oxide-ZnO nanocomposite films with good mechanical, dynamic mechanical, anti-UV and antibacterial properties. J. Chem. Technol. Biotechnol. 90, 1677–1684. https://doi.org/10.1002/jctb.4476
ISO179-1, 2010. Plastics - Determination Of Charpy Impact Properties - Part 1: Non-instrumented Impact Test.
Jiang, L., Zhang, J., Wolcott, M.P., 2007. Comparison of polylactide/nano-sized calcium carbonate and polylactide/montmorillonite composites: Reinforcing effects and toughening mechanisms. Polymer (Guildf). 48, 7632–7644. https://doi.org/10.1016/j.polymer.2007.11.001
K., P., Mohanty, S., Nayak, S.K., 2012. Polylactide/transition metal ion modified montmorillonite nanocomposite-a critical evaluation of mechanical performance and thermal stability. Polym. Compos. 33, 1848–1857. https://doi.org/10.1002/pc.22317
Kontou, E., Georgiopoulos, P., Niaounakis, M., 2012. The role of nanofillers on the degradation behavior of polylactic acid. Polym. Compos. 33, 282–294. https://doi.org/10.1002/pc.21258
Kontou, E., Niaounakis, M., Georgiopoulos, P., 2011. Comparative study of PLA nanocomposites reinforced with clay and silica nanofillers and their mixtures. J. Appl. Polym. Sci. 122, 1519–1529. https://doi.org/10.1002/app.34234
Krikorian, V., Pochan, D.J., 2003. Poly (L-Lactic Acid)/Layered Silicate Nanocomposite: Fabrication, Characterization, and Properties. Chem. Mater. 15, 4317–4324. https://doi.org/10.1021/cm034369+
Lai, S.M., Wu, S.H., Lin, G.G., Don, T.M., 2014. Unusual mechanical properties of melt-blended poly(lactic acid) (PLA)/clay nanocomposites. Eur. Polym. J. 52, 193–206. https://doi.org/10.1016/j.eurpolymj.2013.12.012
Murariu, M., Dubois, P., 2016. PLA composites: From production to properties. Adv. Drug Deliv. Rev. 107, 17–46. https://doi.org/10.1016/j.addr.2016.04.003
Nur-Aimi, M.N., Anuar, H., 2016. Effect of Plasticizer on Fracture Toughness of Polylactic Acid Reinforced with Kenaf Fibre and Montmorillonite Hybrid Biocomposites, in: Nanoclay Reinforced Polymer Composites. pp. 263–280. https://doi.org/10.1007/978-981-10-0950-1
Park, S.D., Todo, M., Arakawa, K., Koganemaru, M., 2006. Effect of crystallinity and loading-rate on mode i fracture behavior of poly(lactic acid). Polymer (Guildf). 47, 1357–1363. https://doi.org/10.1016/j.polymer.2005.12.046

Pirani, S.I., Krishnamachari, P., Hashaikeh, R., 2013. Optimum loading level of nanoclay in PLA nanocomposites: Impact on the mechanical properties and glass transition temperature. J. Thermoplast. Compos. Mater. 27, 1461–1478. https://doi.org/10.1177/0892705712473627

Pluta, M., Paul, M.A., Alexandre, M., Dubois, P., 2006. Plasticized polylactide/clay nanocomposites. I. The role of filler content and its surface organo-modification on the physico-chemical properties. J. Polym. Sci. Part B Polym. Phys. 44, 299–311. https://doi.org/10.1002/polb.20694

Sinha Ray, S., Yamada, K., Okamoto, M., Fujimoto, Y., Ogami, A., Ueda, K., 2003. New polylactide/layered silicate nanocomposites. 5. Designing of materials with desired properties. Polymer (Guildf). 44, 6633–6646. https://doi.org/10.1016/j.polymer.2003.08.021

Stoclet, G., Lefebvre, J.M., Séguéla, R., Vanmansart, C., 2014. In-situ SAXS study of the plastic deformation behavior of polylactide upon cold-drawing. Polym. (United Kingdom) 55, 1817–1828. https://doi.org/10.1016/j.polymer.2014.02.010

Single and hybrid organoclay-filled PLA nanocomposites: Mechanical properties, viscoelastic behavior and fracture toughening mechanism

Jefferson Lopes Alves [a], Paulo de Tarso Vieira e Rosa [b], Vera C. de Redondo Realinho [c], Marcelo de Sousa Pais Antunes [c], José Ignacio Velasco [c], Ana Rita Morales [a*]

[a] School of Chemical Engineering, State University of Campinas, Av. Albert Einstein, 500, 13083-852, Campinas-SP, Brazil
[b] Institute of Chemistry, State University of Campinas, P.O. Box 6154, 13083-970, Campinas-SP, Brazil
[c] Department of Materials Science and Engineering, Poly2 Group, Technical University of Catalonia (UPC BarcelonaTech), ESEIAAT, Colom 11, 08222 Terrassa (Barcelona), Spain
[*] Corresponding author: morales@unicamp.br

Abstract

Poly (lactic acid) (PLA) nanocomposites based on single and hybrid organic-modified montmorillonites were previously studied in terms of their morphological, thermal and fire performance. As surfactants of the organoclays influenced the compatibility between the nanofillers and PLA with different degrees of clay platelets dispersion, the present work investigated the effect of these features in the mechanical properties of PLA nanocomposites. PLA nanocomposites specimens were analyzed by dynamic-mechanical-thermal analysis, which pointed out changes in the viscoelastic behavior of the materials by the incorporation of the organoclays, namely the increase of the storage modulus due to polymer chains movements restriction and reinforcement effects associated with the dispersion of the nanofillers. Flexural and impact testing showed that hybrid organo-montmorillonites containing ester ammonium and ethoxylated amine improved PLA's ductility, toughness and impact resistance. This behavior was explained by the high level of compatibility and interaction between the surfactants and PLA chains due to the polar groups in their structures. These organoclays caused a transition on PLA's fracture from brittle to ductile in a way that the toughening mechanism was explained by crazing and multi-shear banding induced by the plasticized interfacial region around these organoclays.

Keywords: clay, composites, mechanical properties

1. Introduction

Poly (lactic acid) (PLA), a biodegradable thermoplastic, has been gaining ground in medical, durable and non-durable consumer applications, due to issues related to sustainability and the environment. PLA is considered safe for human health (low toxicity), according to the US Food and Drug Administration (FDA) (Garlotta, 2001; Ahmed and Varshney, 2011; Armentano et al., 2013; Castro-Aguirre et al., 2016).

PLA has processing characteristics comparable to conventional thermoplastics (Armentano et al., 2013), and optical, thermal and mechanical properties similar to polypropylene (PP), poly(ethylene terephthalate) (PET), and polystyrene (PS) (Castro-Aguirre et al., 2016); nevertheless, it presents high brittleness, a rather low heat deflection temperature and high gas permeability, limiting its use for packaging purposes (Armentano et al., 2013; Murariu and Dubois, 2016). Many of PLA's limitations, especially mechanical ones such as excessive brittleness, low toughness and low impact resistance, have been minimized by the addition of plasticizers or flexible polymers (Pluta et al., 2006; Balakrishnan et al., 2010; Gunning et al., 2014), organic compounds such as ionic liquids (Chen et al., 2013), and (nano)fillers, as calcium carbonate (Jiang et al., 2007), silica (Kontou et al., 2011, 2012), zinc oxide (Huang et al., 2015), graphene (Bouakaz et al., 2015) and organoclays (Kontou et al., 2011; Fukushima et al., 2013; Pirani et al., 2013; Baouz et al., 2015).

We have previously published the study of the chemical composition effect of different Brazilian organic-modified montmorillonites (OMt) in PLA clay polymer nanocomposites (CPN), as well as the morphology and thermal properties (Alves et al., 2019), and thermal stability and fire performance as a function of the type of organoclay modifier (Alves et al., 2020). Organic-modified montmorillonites with low compatibility with PLA led to the formation of partially-intercalated nanocomposites and microcomposites, while those with good compatibility resulted in partially-intercalated/exfoliated nanocomposites. It was observed that the phosphonium-based montmorillonite was not well dispersed in PLA due to the low compatibility of this surfactant and PLA. On the other hand, hybrid organo-montmorillonite (HOMt) containing di(alkyl ester) dimethyl ammonium chloride (EA) and ethoxylated tallow amine (ETA) as second surfactant promoted better compatibility with PLA due to the presence of polar groups in their structure. The thermal degradation studies also revealed that the thermal stability of PLA nanocomposites was affected by the dispersion of organoclays and that the high amount of phosphonium-containing organoclays caused the

greatest reduction in the thermal stability of the materials due to thermal degradation of PLA chains (Alves et al., 2020).

Dynamic-mechanical-thermal analysis (DMTA) is a technique widely used to study the mechanical and viscoelastic behavior of polymeric materials as a function of temperature. From the DMTA data it is possible to determine the mechanical parameters related with viscoelasticity of the materials, such as the storage modulus (E'), related to the elastic response and stiffness of the material; the loss modulus (E"), related to the viscous response of the material; and the damping factor (tan δ), defined as the ratio between the former (tan δ = E"/E'), which quantifies the energy dissipation capacity of the material. In addition, it is also possible to verify primary (crystallization, melting), secondary (glass transition) and tertiary relaxation transitions. For polymer nanocomposites, one of the main objectives of this technique is to study the changes in these macroscopic properties with nano/microscopic conformational changes of the materials by the addition of nanofillers (Chartoff and Sircar, 2004; Menard and Menard, 2015).

Motivated by these previous works that reported a great innovation in the use of hybrid organoclays based on dual surfactants and the great potential of the PLA nanocomposites developed by these materials for high performance applications, the present work aims to evaluate the effect those different types of OMt on the mechanical and dynamic-mechanical-thermal and fracture mechanism of PLA/OMt nanocomposites, focusing on their developed structures and OMt-PLA interactions.

2. Materials and Methods

2.1. Materials

Single and hybrid organically-modified montmorillonites modified by a semi-solid method with different kinds of surfactants, namely di-(hydrogenated tallow) dimethyl ammonium chloride (HTA), trihexyl tetradecyl phosphonium chloride (TDP), di(alkyl ester) dimethyl ammonium chloride (EA) and ethoxylated tallow amine (ETA), were used to prepare nanocomposites based on a PLA (Ingeo 3052D) supplied by NatureWorks LLC with a D-lactide content around 4%. The materials and methods used to prepare the different organic-modified montmorillonites are described in previous works (Alves et al., 2016, 2017, 2018). For

comparison purposes, commercial organoclays Cloisite 20A and Cloisite 30B, supplied by Southern Clay Products, were used.

2.2. Samples preparation

A counter-rotating internal mixer (Brabender Plasti-Corder® W50EHT) was used to prepare PLA masterbatches with 20 wt% of organoclay, and a co-rotating twin screw extruder (Collin Kneter 25X36D), with diameter of 25 mm and L/D of 36 was used to dilute the masterbatches, producing clay PLA nanocomposites with 2 wt%, 6 wt% and 8 wt%. More details about the preparation method are given in a previous work (Alves et al., 2019). Virgin PLA was extruded at the same conditions and labeled as EPLA. A description of all material samples with their respective organoclay type(s) and content used to prepare the PLA nanocomposites is summarized in **Table 1**.

Table 1. Composition of PLA nanocomposites.

CPN code	Organoclay [(1)]	Organoclay content (wt%)	Surfactant type [(1)] and amount [(2)]
PN2MHTA	MHTA	2	HTA
PN6MHTA		6	
PN8MHTA		8	
PN2MTDP	MTDP	2	TDP
PN6MTDP		6	
PN8MTDP		8	
PN2HMPHTA	HMPHTA	2	14 wt% of TDP / 17 wt% of HTA
PN6HMPHTA		6	
PN8HMPHTA		8	
PN2HMPEA	HMPEA	2	12 wt% of TDP / 20 wt% of EA
PN6HMPEA		6	
PN8HMPEA		8	
PN2HMPETA	HMPETA	2	18 wt% of TDP / 9 wt% of ETA
PN6HMPETA		6	
PN8HMPETA		8	

PN2C30B		2	
PN6C30B	C30B	6	MT2EtOH
PN8C30B		8	
PN2C20A		2	
PN6C20A	C20A	6	HTA
PN8C20A		8	

(1) HTA: Dihydrogenated tallow dimethyl quaternary ammonium ion. TDP: Trihexyl tetradecyl quaternary phosphonium. EA: Dialkyl ester dimethyl quaternary ammonium ion. ETA: Ethoxylated tallow amine. MT2EtOH: Methyl tallow bis-2-hydroxyethyl quaternary ammonium ion.
(2) Surfactant amount determined by TGA (in nitrogen atmosphere).

2.3. Characterization procedure

Dynamic-mechanical-thermal analysis (DMTA) was carried out using a TA Instruments Q800 apparatus, in single cantilever mode, with a constant strain of 0.02% and frequency of 1 Hz, from 30 to 145 °C at 2 °C/min, using a minimum of two specimens with typical dimensions of 35.6 mm (length) × 12.7 mm (width) × 3.0 mm (thickness).

The flexural properties were determined by three-point bending according to standard ISO 178, using a Galdabini Sun 2500 equipment with a load cell of 5 kN. Tests were performed at room temperature using a minimum of four specimens per material, with typical dimensions of 60.0 mm (length) × 10.0 mm (width) × 3.0 mm (thickness), under a constant velocity of 5 mm/min.

The impact properties were determined by Charpy impact testing using a Zwick HIT 5.5P equipment according to standard ISO 179-1. The tests were carried out using a hammer with a maximum amount of energy of 1 J with perpendicular impact to the thinner face of both notched and un-notched specimens; a minimum of three specimens per material, with typical dimensions of 80.0 mm (length) × 10.0 mm (width) × 4.0 mm (thickness), were used. The notch was made with a radius of 0.25 mm and depth of 2.0 mm (type A).

Scanning Electron Microscopy (SEM) was used to study the morphology and the fracture behavior of the fractured surfaces of three-point bending and impact specimens. The images were obtained using a JEOL JSM-5610 microscope applying a voltage of 15 kV and a

working distance of 30 mm. The samples were prepared at room temperature by depositing a thin layer of gold on the fractured surface using a BAL-TEC SCD005 sputter coater (argon atmosphere).

3. Results and discussion

3.1. Dynamic-mechanical-thermal properties

Characteristic curves of the evolution of the storage modulus (E'), loss modulus (E") and tan δ with temperature are shown in **Figure 1**. CPN materials displayed T_g values slightly lower than EPLA. The increase in T_g observed in E' curves and the decrease in tan δ curves above 95 °C are associated to the cold crystallization of PLA. The results summarized in **Table 2** feature a gradual decrease in the onset of cold crystallization temperature ($T_{cc.onset}$) of PLA by the addition of all OMt. These results were similar to the ones determined by the first heating in DSC results (Alves et al., 2019).

Analyzing the glassy plateau (E' at 30°C in **Figure 1** and in **Table 2**), it can be seen that the storage modulus of most of the materials was slightly enhanced by increasing OMt content. The enhancement was more pronounced in nanocomposites containing C30B, C20A, MHTA and HMPEA. The increment in E' with OMt content is associated with the reinforcing effect offered by the dispersed rigid-structures (Krikorian and Pochan, 2003; Sinha Ray et al., 2003; Kontou et al., 2011). The enhancement effect depends on the dispersion degree of the nanostructures, as well as the interfacial interaction between the phases (Sinha Ray et al., 2003; Kontou et al., 2011). Therefore, these results are in agreement with structural and morphological analyses presented in previous work (Alves et al., 2019), justifying the higher storage modulus of PLA nanocomposites with C30B.

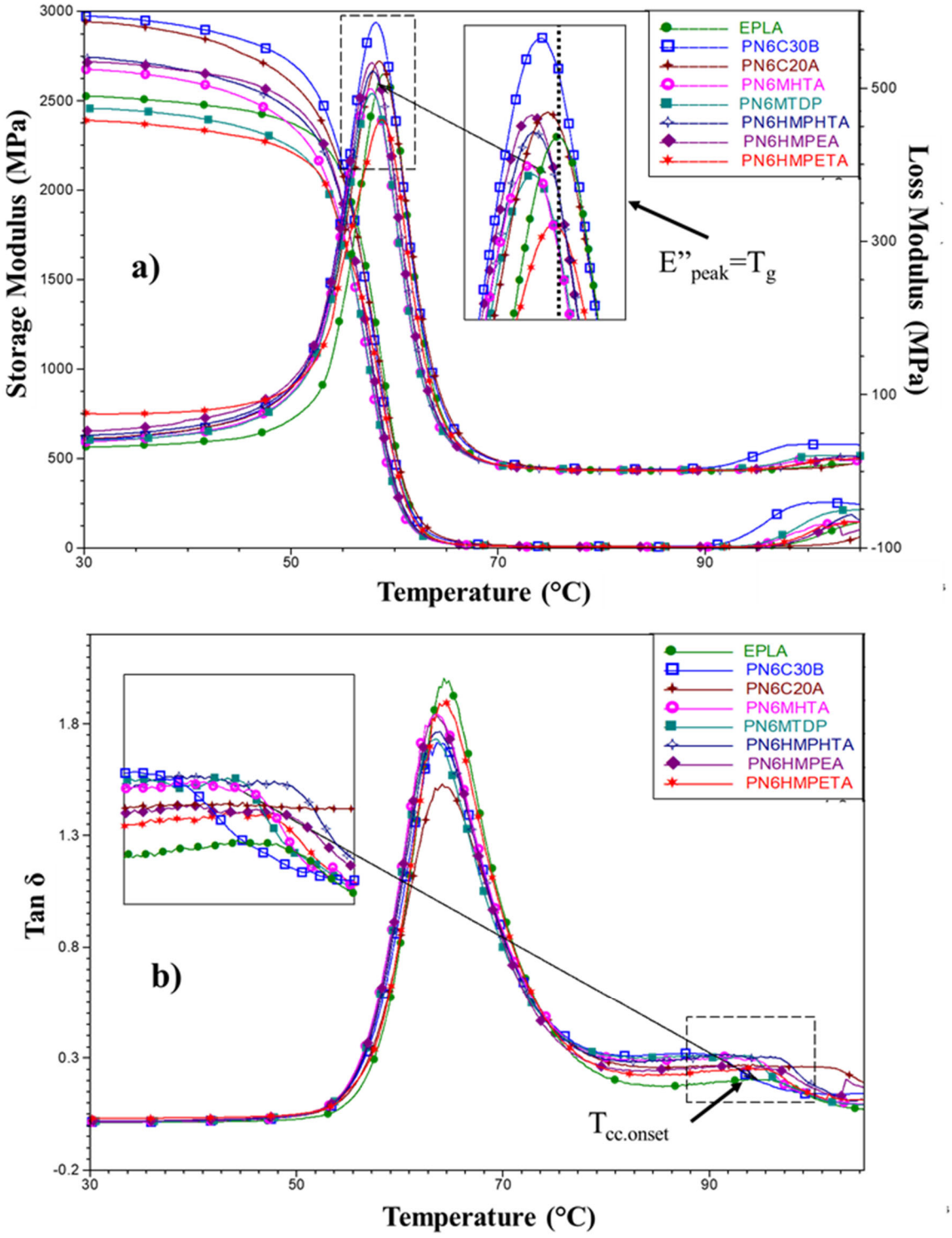

Figure 1. Representative curves of the evolution of the (a) storage modulus (E') and loss modulus (E''), and (b) tan δ with temperature for PLA and CPN with 6 wt% of OMt.

Table 2. Glass transition temperature (T_g), onset of cold crystallization temperature ($T_{cc.onset}$) and storage modulus of PLA nanocomposites.

CPN code	T_g (°C) (1)	$T_{cc.onset}$ (°C) (2)	E' (MPa) (3)

PLA	60	97	2562
PN2MHTA	58	96	2673
PN6MHTA	58	95	2738
PN8MHTA	58	93	2812
PN2MTDP	59	94	2588
PN6MTDP	58	94	2500
PN8MTDP	57	91	2639
PN2HMPHTA	58	96	2536
PN6HMPHTA	58	96	2771
PN8HMPHTA	58	94	2783
PN2HMPEA	58	93	2674
PN6HMPEA	58	95	2733
PN8HMPEA	58	97	2798
PN2HMPETA	59	92	2575
PN6HMPETA	59	95	2510
PN8HMPETA	59	94	2561
PN2C30B	59	90	2626
PN6C30B	58	91	3112
PN8C30B	57	91	3298
PN2C20A	59	96	2599
PN6C20A	59	102	2921
PN8C20A	58	100	3027

(1) T_g determined at the maximum of the loss modulus curve.
(2) $T_{cc.onset}$ determined at the second peak of the tan δ curve.
(3) Storage modulus determined at 30 ºC.

PLA nanocomposites prepared with MTDP and HMPETA caused nearly no change in E', which can be associated to the reduction of molecular mass by thermal degradation during extrusion, as suggested by TGA and GPC discussion in previous work (Alves et al., 2020). Furthermore, it was reported that at high OMt content the chain confinement effect can be reduced and there is a reduction of the fillers/matrix contact area due to an increase in the number of OMt agglomerates (Kontou et al., 2011, 2012; Pirani et al., 2013). Indeed, the increase of C30B content from 2 wt% to 6 wt% caused a significant increase in E' for PNC30B nanocomposites, but the same was not observed for 8 wt%.

3.2. Flexural properties

PLA is well known for its excessive brittleness. The improvement of the toughness of PLA without loss of other properties, such as elastic modulus or thermal stability, has been the

aim of several studies (Jiang et al., 2007; K. et al., 2012; Baouz et al., 2015; Nur-Aimi and Anuar, 2016). Flexural and impact tests were performed on EPLA and PLA nanocomposites aiming to evaluate the influence of OMt's type and content on the mechanical performance of PLA nanocomposites.

The flexural stress-strain curves of PLA nanocomposites are presented in **Figure 2**, the variation of the flexural modulus and strength in **Figure 3**, and the variation of the flexural strain and toughness in **Figure 4**. The flexural modulus and flexural strength of PLA nanocomposites exhibited a contrary trend regarding OMt's content. Overall, the flexural modulus slightly increased by the addition of all OMt, and by increasing their concentration, whereas the flexural strength gradually decreased.

Generally speaking, the flexural modulus of PLA nanocomposites displayed a similar trend as the storage modulus presented in the prior section. The enhancement of the flexural modulus observed for the nanocomposites when compared with EPLA is due to the reinforcement effect of the dispersed nanoclay structures in the matrix, acting as rigid fillers absorbing and supporting the external mechanical load. This enhancement was less pronounced when using MTDP and the three HOMts – MPHTA, MPEA and MPETA, which can be associated with molar mass reduction, as reported in a previous work (Alves et al., 2020), probably due to the high phosphonium salt content in these materials, which showed to be quite incompatible with PLA matrix (Alves et al., 2019, 2020). The increase of the modulus with augmenting OMt content may be associated to the presence of small clay stacks/agglomerates well distributed throughout the matrix that can influence the stiffness more than exfoliated structures (Lai et al., 2014). The occurrence of those microstructures (agglomerates of clay stacks) was observed in TEM micrographs and shown in a previous work (Alves et al., 2019). They do not provide sufficient interfacial interactions/adhesion between the phases, which can lead to an easy debonding of these particles from the matrix at lower stress, even lower than the yield point of the matrix. Such structures acted as defects and stress concentrators, creating localized weakening points that reduced the material strength (LAI et al., 2014), supporting the the evolution of the flexural strength with OMt's content.

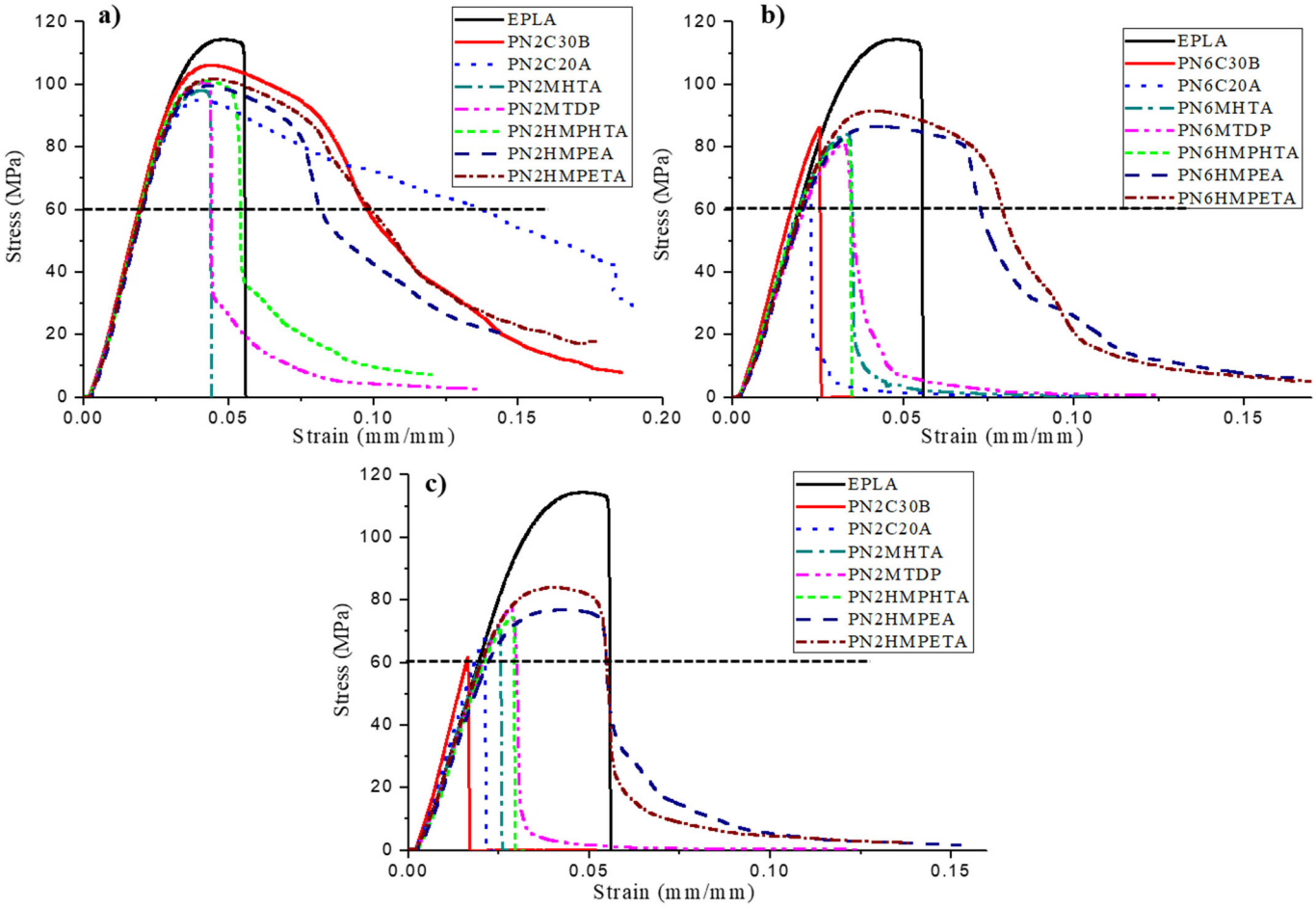

Figure 2. Flexural stress-strain curves of PLA nanocomposites with (a) 2 wt%, (b) 6 wt% and (c) 8 wt% of OMt.

The flexural strain at break was not easy to determine as can be seen in **Figure 2**, as in some cases the material did not break or it was difficult to identify in the curve. Thus, to evaluate the elongation behavior of the materials, the maximum flexural strain was determined at the stress drop at 60 MPa (indicated in **Figure 2**). The flexural strain and toughness, determined as the area below the stress-strain curve, are presented in **Figure 4**. In general, both properties followed the same trend. EPLA displayed a typical brittle-like mechanical behavior, breaking with nearly no plastic deformation at 5.5% of strain with a toughness of 4.5 MJ/m^3. The addition of most of the organoclays, mainly at high content, increased the brittleness of PLA, as can be seen by the flexural strain and toughness results.

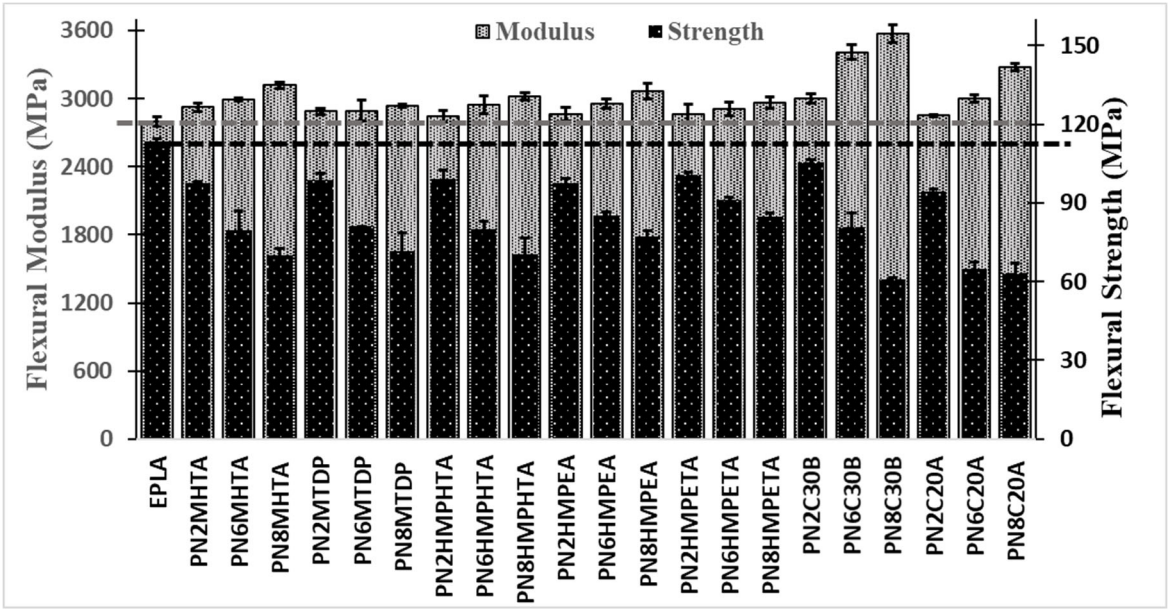

Figure 3. Evaluation of the flexural modulus and flexural strength with OMt type and content. Dotted lines indicate the values of EPLA.

The ductility of PLA was significantly enhanced by adding 2 wt% of MPEA, MPETA, C30B and C20A, which led to an increase in the flexural strain of around 10% and in the toughness of around 8 MJ/m^3. However, looking to the CPN series with C30B and C20A (**Figure 4**), when the OMt content raised to 6 wt% and 8 wt%, both the flexural strain and the toughness drastically dropped to values lower than those of EPLA. These materials fractured in a completely brittle manner without yielding **(Figure 2**). Lai et al. (2014) reported a large elongation at break under tensile testing of more than 200% in PLA nanocomposites with only 1 phr of C30B, which drastically decreased to values lower than that of PLA by increasing OMt's content to 3 and 5 phr. This same trend was also found by Acik et al. (2016), which observed an enhancement of the tensile elongation of PLA/C30B nanocomposites with 1 wt% to 3 wt% of organoclays and a drastic drop after 4 wt%. In contrast with these studies, this work shows that the content increase of the two hybrid OMts, HMPEA and HMPETA, caused a lighter reduction of these properties when compared to other organoclays. For a content of 6 wt% the flexural strain was higher than PLA's at around 7.0% and 9.5%, and toughness was 5 MJ/m^3 and 6.2 MJ/m^3, respectively for MPEA and MPETA. This can be associated to a plasticizing effect caused by the good dispersion and good interfacial interaction of these organoclays with PLA provided by the EA and ETA surfactants used in these hybrid OMts, improving toughness. For a content of 8 wt% of these organoclays, the strain was almost the same as PLA's and the toughness was slightly reduced. Besides, plastic deformation can still be observed in the curves of these nanocomposites (see **Figure 2c**).

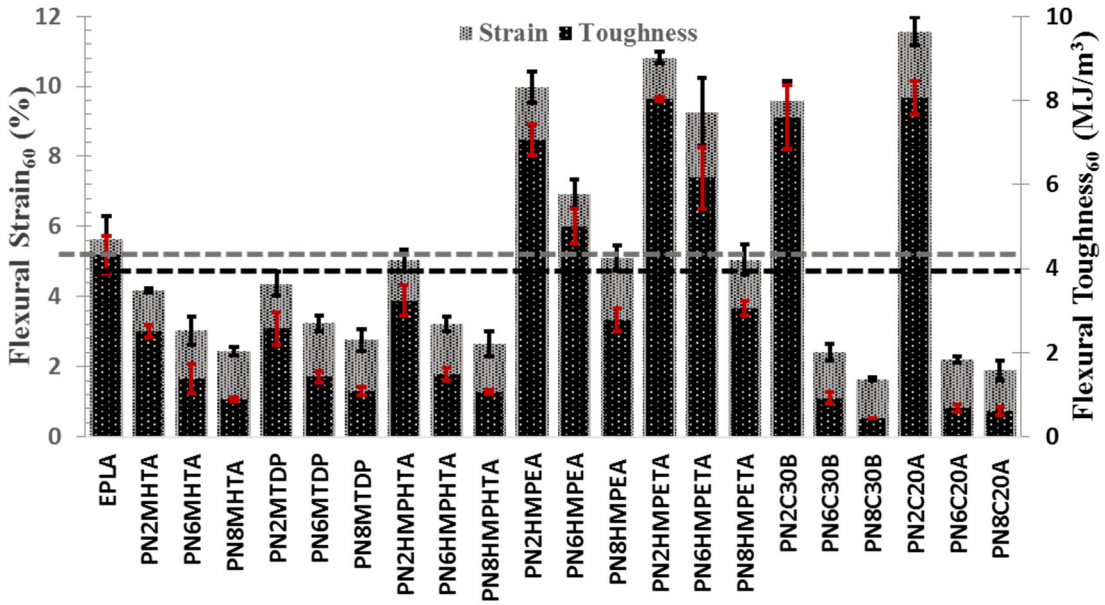

Figure 4. Evaluation of the flexural strain and flexural toughness at a stress of 60 MPa with OMt type and content. Dotted lines indicate the values of EPLA.

3.3. Impact properties

The results of the impact resistance are shown in **Figure 5**. Nearly no improvement in un-notched and notched impact resistance was achieved by adding most of the organoclays, in some cases the impact resistance decreasing with augmenting OMt's content.

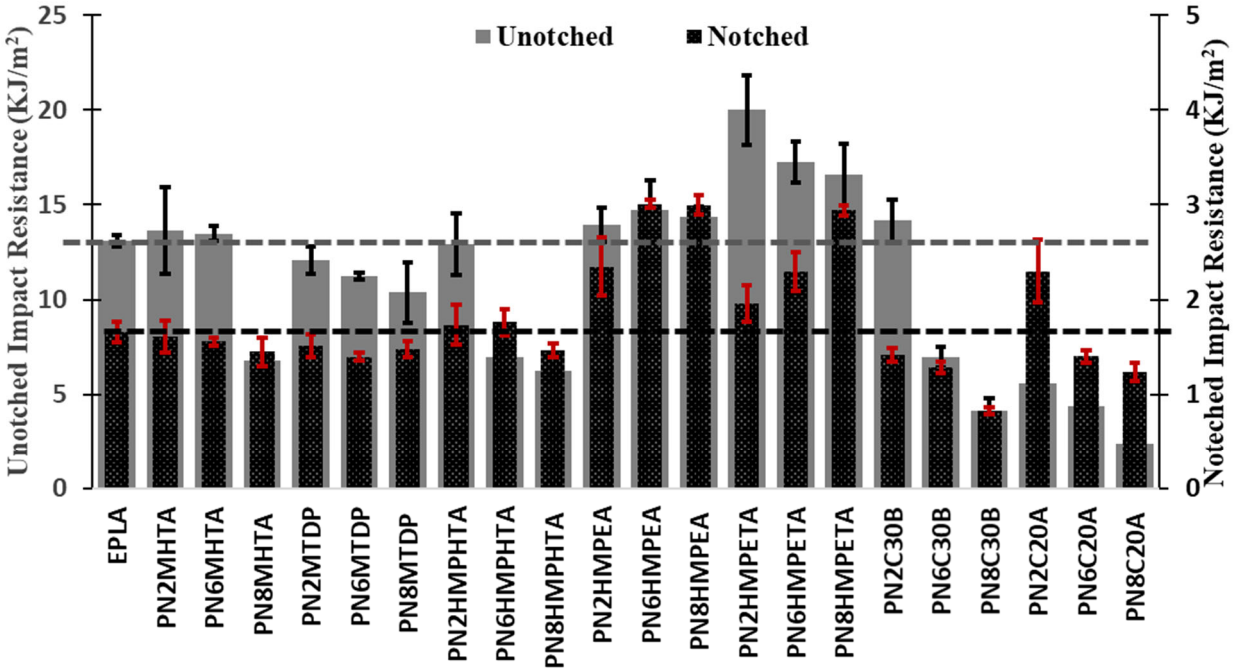

Figure 5. Evaluation of the impact resistance with organic-modified montmorillonites (OMt) type and content. Dotted lines mark the values of EPLA.

A great enhancement, comparing with EPLA, was achieved for PLA nanocomposites with HMPEA and HMPETA. The un-notched impact resistance of these materials slightly decreased with OMt's content, whereas the notched ones surprisingly improved with OMt's content. This mechanical property strongly depends on the dispersion degree of nanoparticles as well as the interfacial interaction between phases. The gradual decrease of the un-notched impact resistance can be explained by the large microstructures formed by increasing the amount of OMt, which acted as local stress concentrators that favored the initial crack formation by debonding/cavitation of these microparticles at lower critical stress/energy. On the other hand, crack propagation depends on the adhesion and dispersion degree of the micro and nanostructures in the matrix. Thus, in the case of notched specimens, the notch acted as initial crack, which means that enhancement in the impact resistance was associated to a good dispersion and interfacial interaction between HMPEA/HMPETA and PLA, which allowed an effective stress transfer from the matrix to the fillers and a barrier effect that limited crack propagation. Therefore, PLA nanocomposites with HMPEA/HMPETA had their toughness and impact resistance enhanced due to the good dispersion of the nanoparticles and strong interaction with PLA, as suggested by Alves et al. (2019).

Albeit PN2C20A nanocomposites presented a notched impact resistance higher than that of EPLA, it substantially decreased with augmenting OMt's content to values lower than EPLA. Surprisingly, blending PLA with 2 wt% of C30B caused nearly no enhancement in the impact resistance and drastically decreased with further increasing OMt's content. It was expected that this property, alongside flexural toughness, would increase with at least 2 wt% of C30B due to the good dispersion of C30B and good interaction between PLA and C30B.

3.4. Toughening mechanism and morphology of the fracture surface

Flexural and impact results provided information that the dispersion of the different types of organoclay affected the mechanical behavior of PLA. Even at high content, HMPEA and HMPETA caused a transition on PLA deformation behavior from mainly brittle or quasi-brittle to ductile. The mechanisms of energy absorption in brittle polymers has been widely

discussed in the literature and strongly associated to catastrophic crack propagation and crazing (Park et al., 2006; Jiang et al., 2007; Stoclet et al., 2014; Baouz et al., 2015; Nur-Aimi and Anuar, 2016). Crazing is a localized cavitational mechanism characterized by the formation of interpenetrating microvoids bridged by polymer fibrils (fine filaments formed by molecules of the stretched backbone polymer chains) in a region of the material under high localized tensile stress and/or yielding. Fibrils act as anchors hindering crack spread and, depending on the applied tensile stress, microvoids growth and coalesced forming cracks until the material ruptures (Stoclet et al., 2014; Nur-Aimi and Anuar, 2016).

Macroscopic stress whitening zone in the zone under tensile loading (opposite side of load application) was reveled in the flexural specimens of some nanocomposites, mainly the ones that presented plastic deformation behavior observed in **Figure 2**. Such characteristics can be seen in **Figure 6**.

EPLA's specimen ruptured in a brittle manner into two portions with no sign of plastic deformation. On the other hand, all nanocomposite specimens with HMPEA and HMPETA displayed a whitening region, typically associated to a crazing mechanism, and did not completely break into two portions until the maximum elongation used in the tests of around 20%. To reach such accomplishments, a high extent of well-dispersed nanofillers with high aspect ratio is necessary, besides a high compatibility between polymer and clay modifier, in order to allow interfacial interaction (Jiang et al., 2007; Baouz et al., 2015; Nur-Aimi and Anuar, 2016). This explanation supports the morphology and the change in fracture behavior by blending PLA with the hybrid HMPEA and HMPETA organoclays, even at high concentration.

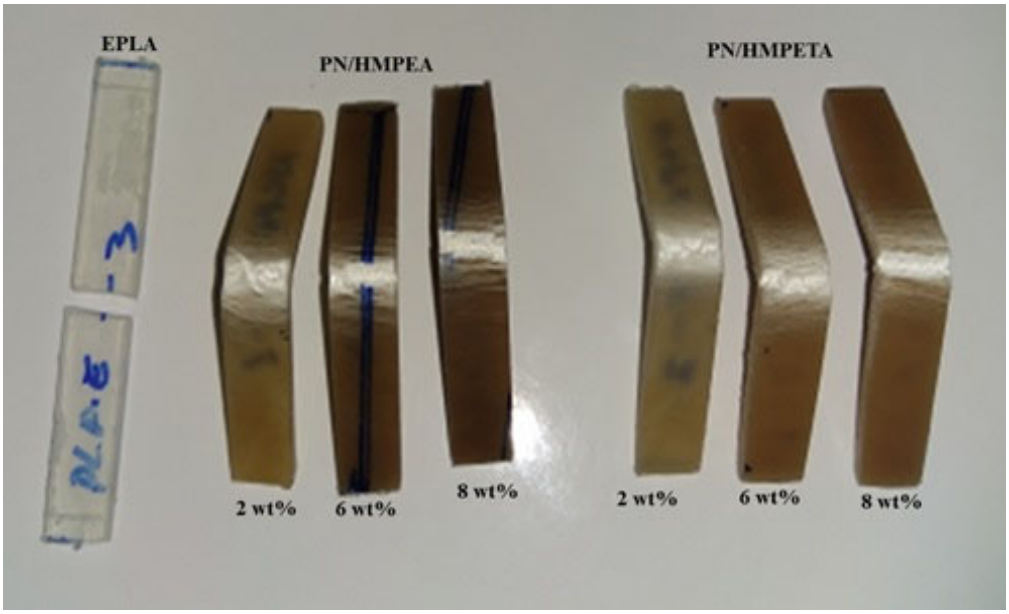

Figure 6. Specimens of EPLA and PLA nanocomposites with HMPEA and HMPETA after flexural testing showing whitening of the crazed region.

The fracture surface of some flexural specimens studied by SEM can be seen in **Figure 7** and in **Figure 8**. The SEM micrograph of EPLA shows a smooth surface with nearly no sign of plastic deformation, which confirmed that PLA sample broke quickly due to fast development and propagation of critical cracks. PLA nanocomposites with 2 and 8 wt% of MTDP, which also featured nearly no yielding during flexural stress, exhibited a slight rough surface without microvoiding and almost no plastic deformation (**Figure 7b** and **Figure 7c**). A large amount of flaws from cavitation and debonding due to OMt agglomerates can be seen in the fracture surface, which confirmed the poor adhesion and low ductility promoted by this organoclay. On the other hand, the samples that displayed large yielding and intense stress whitening, as PN2C30B (**Figure 7d** and **Figure 7e**), PN2HMPEA (**Figure 8a** and **Figure 8b**) and PN2HMPETA (**Figure 8d** and **Figure 8e**), showed extensive plastic deformation (micrographs at low magnification). It happened due to a large amount of small microvoids surrounded by extensively oriented ligaments. That may be fibrils that were drawn out from the polymer under flexural stress, as can be seen in the micrographs at high magnification. It features that a lot of energy was absorbed before failure of these materials since these kind of mechanisms are associated to extensive local plastic deformation that leads to a larger strain-at-break and higher toughness.

Flexural curves suggested that the strength and toughness of PLA was negatively affected when the concentration of OMt increased, and the reason for that can be elucidated by

SEM micrographs of PLA nanocomposites with 8 wt% as presented in **Figure 7f**, **Figure 8c** and **Figure 8f**. The fracture surface of PN8C30B shows large voids/flaws associated with tactoids/agglomerates of clay particles and sign of waves from crack propagation. This suggests that the catastrophic failure of the material was caused by debonding of these microstructures that acted as stress concentrators, resulting in early critical crack formation and quick propagation. OMt clusters and cavities associated with microparticles debonding could also be seen by analyzing the fracture surface of nanocomposites with 8 wt% of HMPEA and HMPETA. However, these materials presented greater plastic deformation and no clear waves of crack propagation when compared to the samples with C30B. Indeed, these microsize structures led to the early fracture of the material with less energy than the ones with 2 wt%, but the good interaction of these organoclays still promoted microvoiding and shear band (plastic deformation), resulting in a more ductile material.

More information about the fracture toughening mechanisms could be obtained by analyzing the fracture surface of notched impact specimens, as presented in **Figure 9** and **Figure 10**. For EPLA (**Figure 9**) clear waves in the notch direction were found. This surface was characterized by a smooth surface with stress whitening due to fast matrix detachment, resulting in polymer fibrillation without microvoiding, as seen in the high magnification micrograph. Such morphology suggests that EPLA suffered an abrupt rupture under impact stress due to fast crack propagation with very low energy values.

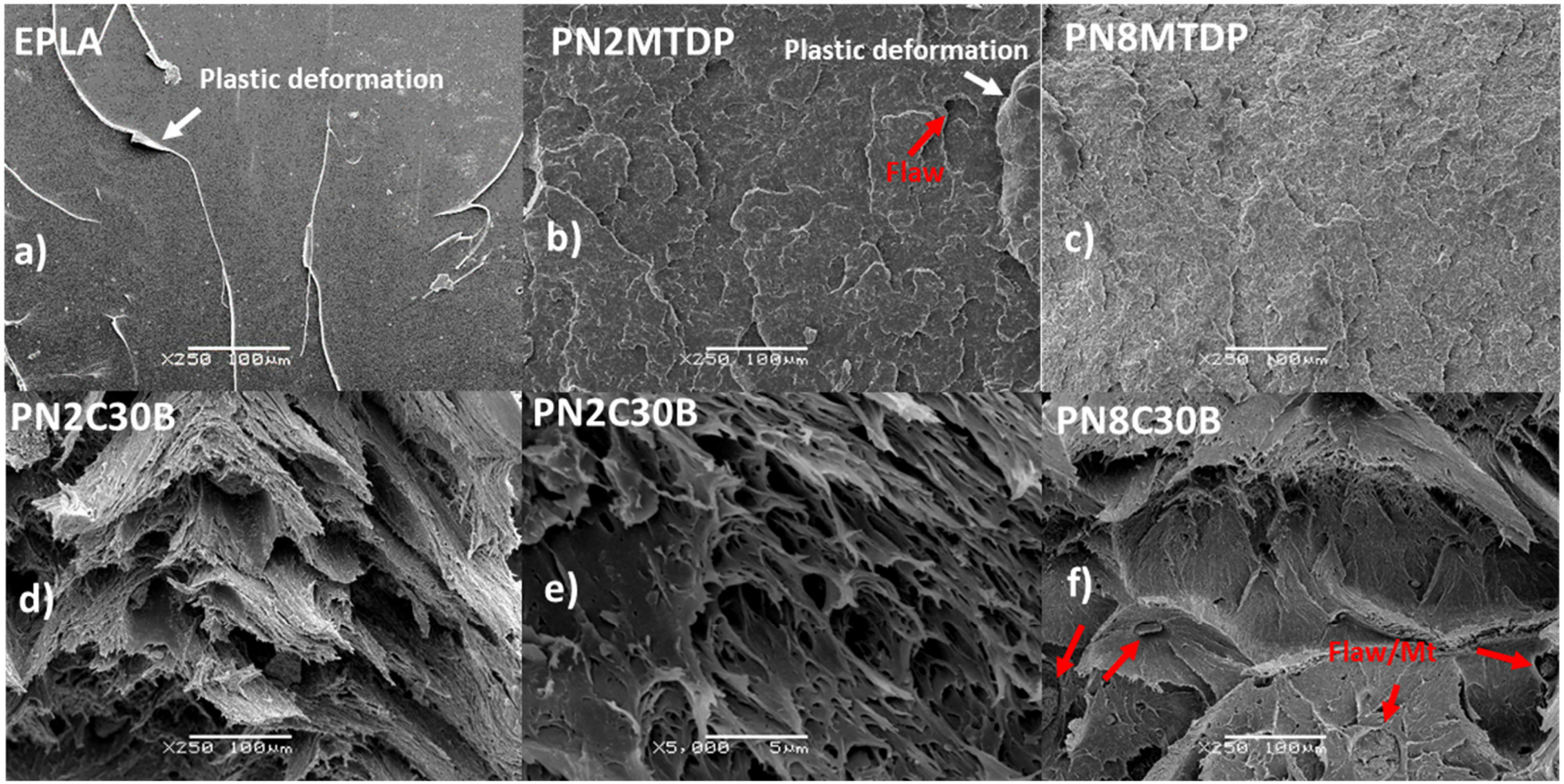

Figure 7. SEM micrographs of the fracture surfaces of flexural specimens: (a) EPLA, (b) PN2MTDP, (c) PN8MTDP, (d) PN2C30B at low magnification, (e) PN2C30B at high magnification and (f) PN8C30B.

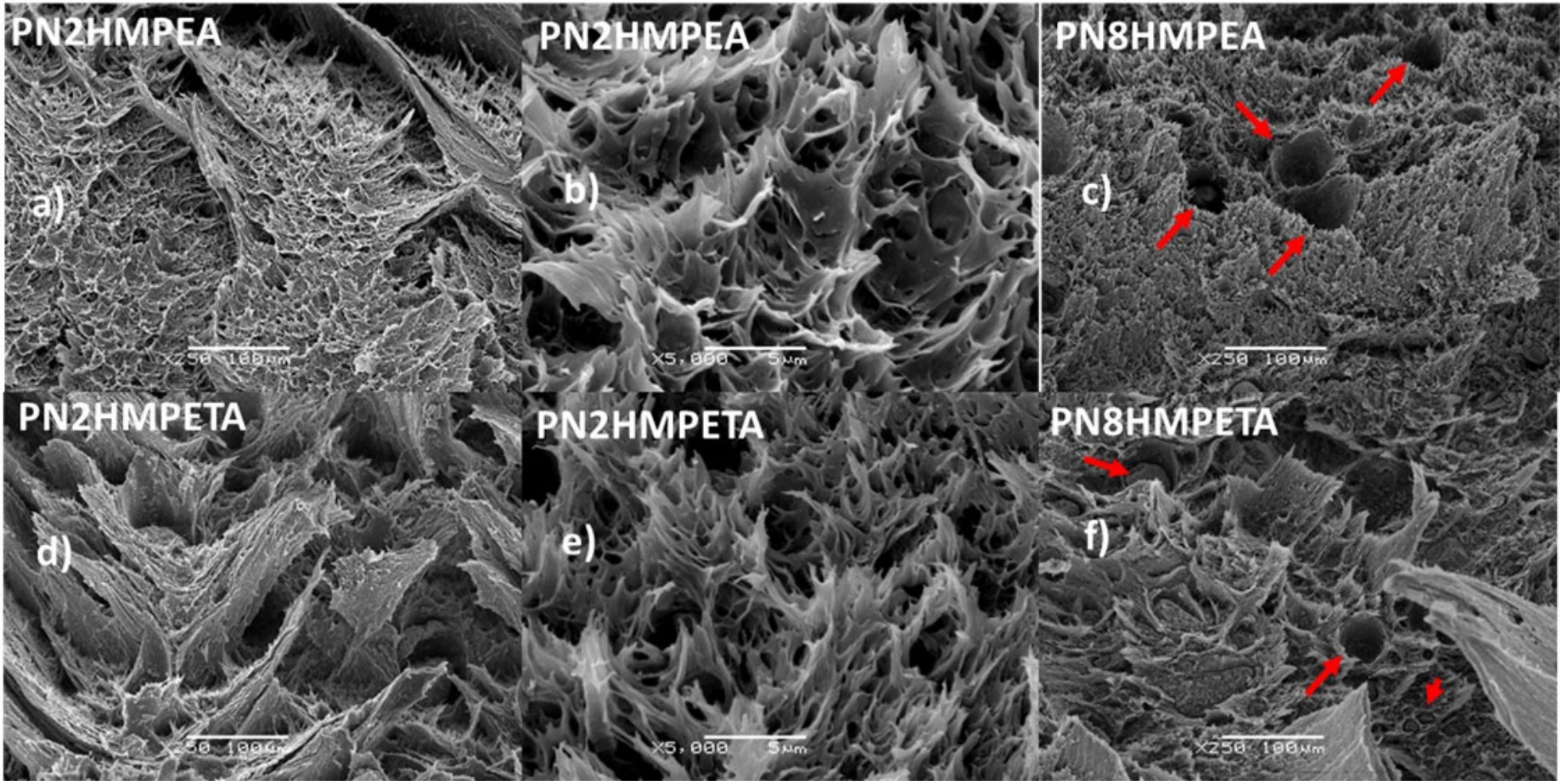

Figure 8. SEM micrographs of the fracture surfaces of flexural specimens: (a) PN2HMPEA at low magnification, (b) PN2HMPEA at high magnification, (c) PN8HMPEA, (d) PN2HMPETA at low magnification, (e) PN2HMPETA at high magnification and (f) PN8HMPETA.

As well as in flexural specimens, the impact fracture of PLA nanocomposites with HMPEA and HMPETA (**Figure 10**) exhibited a rougher surface than EPLA. The roughness on the fracture surface of both materials increased with augmenting OMt's content. The high magnification micrographs revealed an increasing in extent of microvoids and plastic deformation (fibrils) with OMt content. This behavior indicates that crazing and shear yielding mechanisms increased with HMPEA and HMPETA concentration. It was probably induced by the higher amount of well-dispersed and adhered stacks and platelets of OMt, which led to the enhancement of the material toughness under impact load as exhibited in **Figure 5**. Indeed, some OMt stacks can be seen well anchored to the matrix and embedded within the PLA matrix enveloped by microvoids on the fracture surface of PLA nanocomposites with 2 and 8 wt% of HMPEA (**Figure 10a'** and **Figure 10b'**). Thus, high energy was necessary to create these surfaces and to fracture these materials, which resulted in the enhancement of fracture toughness under impact test.

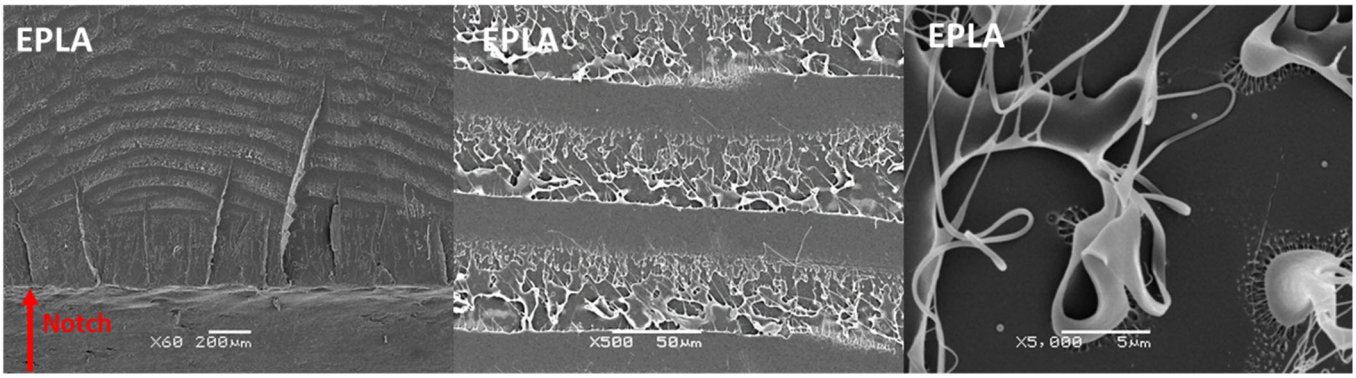

Figure 9. SEM micrographs of the fracture surfaces of notched impact specimens of EPLA at low, medium and high magnification.

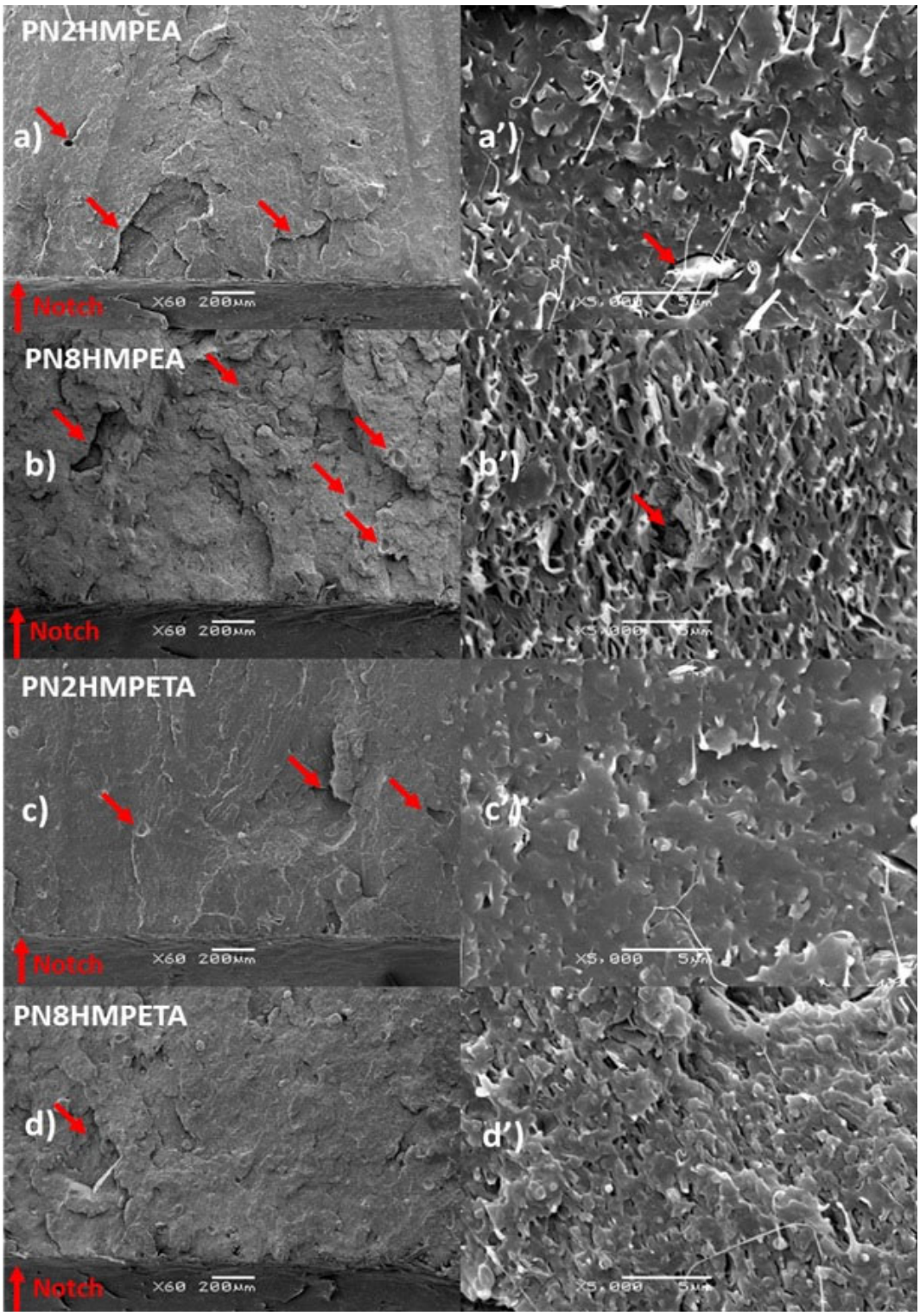

Figure 10. SEM micrographs of the fracture surfaces of notched impact specimens: (a) low and high magnification PN2HMPEA, (b) low and high magnification PN8HMPEA, (c) low and high magnification PN2HMPETA and (d) low and high magnification PN8HMPETA.

The fracture behavior of PLA was in fact influenced by OMt's chemical composition and concentration. The toughness of PLA, as suggested by flexural and impact tests, was mainly increased

when adding HMPEA and HMPETA due to its good dispersion and interfacial interaction. Such morphology created physical barriers to the coalescence of crazes and crack propagation, diverting it in random directions. In addition, the partially-exfoliated nanostructure, coupled with the PLA by strong interactions, allowed an effective matrix toughness increase by crazing and multi-shear banding mechanisms, induced by a highly plasticized interfacial region around the nanoclays (Lai et al., 2014).

4. Conclusions

The effect of organic-modified montmorillonites chemical composition on the morphological, thermal and mechanical properties of PLA nanocomposites was studied. DMTA, flexural and impact testing provided evidences that the degree of compatibility between the clay modifiers and PLA governs the morphology of PLA nanocomposites and consequently affects their mechanical properties.

The hybrid organo-montmorillonites containing ester ammonium (EA) and ethoxylated amine (ETA) promoted a high level of compatibility and interaction with PLA due to polar groups in their structures, enhancing the ductility and impact resistance of PLA nanocomposites. The toughening mechanism of PLA nanocomposites containing these organoclays was enhanced due to its good dispersion and strong interfacial interactions between the phases, which promoted localized plastic deformation induced by crazing and shear band mechanisms.

Acknowledgments

The authors acknowledge the Brazilian National Council of Scientific and Technological Development (CNPQ) [grant numbers: 142448/2013-3, 232751/2014-5] and the Spanish Ministry of Science and Innovation for the financial support of project MAT2017-89787-P.

References

Acik, E., Orbey, N., Yilmazer, U., 2016. Rheological properties of poly(lactic acid) based nanocomposites: Effects of different organoclay modifiers and compatibilizers. J. Appl. Polym. Sci. 133, 42915. https://doi.org/10.1002/app.42915

Ahmed, J., Varshney, S.K., 2011. Polylactides—Chemistry, Properties and Green Packaging Technology: A Review. Int. J. Food Prop. 14, 37–58. https://doi.org/10.1080/10942910903125284

Alves, J.L., Rosa, P. de T.V. e., Realinho, V., Antunes, M., Velasco, J.I., Morales, A.R., 2020. The effect of Brazilian organic-modified montmorillonites on the thermal stability and fire performance of organoclay-filled PLA nanocomposites. Appl. Clay Sci. 194, 105697.

https://doi.org/10.1016/j.clay.2020.105697
Alves, J.L., Rosa, P. de T.V. e., Realinho, V., Antunes, M., Velasco, J.I., Morales, A.R., 2019. Influence of chemical composition of Brazilian organoclays on the morphological, structural and thermal properties of PLA-organoclay nanocomposites. Appl. Clay Sci. 180, 105186. https://doi.org/10.1016/j.clay.2019.105186
Alves, J.L., Rosa, P. de T.V. e, Morales, A.R., 2018. Hybrid organo-montmorillonite produced by simultaneous intercalation of phosphonium and ammonium/amine based surfactants. Mater. Chem. Phys. 218, 279–288. https://doi.org/10.1016/j.matchemphys.2018.07.040
Alves, J.L., Rosa, P. de T.V. e, Morales, A.R., 2017. Evaluation of organic modification of montmorillonite with ionic and nonionic surfactants. Appl. Clay Sci. 150, 23–33. https://doi.org/10.1016/j.clay.2017.09.001
Alves, J.L., Rosa, P.D.T.V.E., Morales, A.R., 2016. A comparative study of different routes for the modification of montmorillonite with ammonium and phosphonium salts. Appl. Clay Sci. 132–133, 475–484. https://doi.org/10.1016/j.clay.2016.07.018
Armentano, I., Bitinis, N., Fortunati, E., Mattioli, S., Rescignano, N., Verdejo, R., Lopez-Manchado, M. a., Kenny, J.M., 2013. Multifunctional nanostructured PLA materials for packaging and tissue engineering. Prog. Polym. Sci. 38, 1720–1747. https://doi.org/10.1016/j.progpolymsci.2013.05.010
Balakrishnan, H., Hassan, A., Wahit, M.U., Yussuf, A.A., Razak, S.B.A., 2010. Novel toughened polylactic acid nanocomposite: Mechanical, thermal and morphological properties. Mater. Des. 31, 3289–3298. https://doi.org/10.1016/j.matdes.2010.02.008
Baouz, T., Acik, E., Rezgui, F., Yilmazer, U., 2015. Effects of mixing protocols on impact modified poly(lactic acid) layered silicate nanocomposites. J. Appl. Polym. Sci. 132, 1–14. https://doi.org/10.1002/app.41518
Bouakaz, B.S., Pillin, I., Habi, A., Grohens, Y., 2015. Synergy between fillers in organomontmorillonite/graphene-PLA nanocomposites. Appl. Clay Sci. 116–117, 69–77. https://doi.org/10.1016/j.clay.2015.08.017
Castro-Aguirre, E., Iñiguez-Franco, F., Samsudin, H., Fang, X., Auras, R., 2016. Poly(lactic acid)—Mass production, processing, industrial applications, and end of life. Adv. Drug Deliv. Rev. https://doi.org/10.1016/j.addr.2016.03.010
Chen, B.-K., Wu, T.-Y., Chang, Y.-M., Chen, A.F., 2013. Ductile polylactic acid prepared with ionic liquids. Chem. Eng. J. 215–216, 886–893. https://doi.org/10.1016/j.cej.2012.11.078
Fukushima, K., Tabuani, D., Arena, M., Gennari, M., Camino, G., 2013. Effect of clay type and loading on thermal, mechanical properties and biodegradation of poly(lactic acid) nanocomposites. React. Funct. Polym. 73. https://doi.org/10.1016/j.reactfunctpolym.2013.01.003
Garlotta, D., 2001. A Literature Review of Poly(Lactic Acid). J. Polym. Environ. 9, 63–84.

https://doi.org/10.1023/A:1020200822435
Gunning, M.A., Geever, L.M., Killion, J.A., Lyons, J.G., Chen, B., Higginbotham, C.L., 2014. The effect of the mixing routes of biodegradable polylactic acid and polyhydroxybutyrate nanocomposites and compatibilised nanocomposites. J. Thermoplast. Compos. Mater. 1–20. https://doi.org/10.1177/0892705714526912
Huang, Y., Wang, T., Zhao, X., Wang, X., Zhou, L., Yang, Y., Liao, F., Ju, Y., 2015. Poly(lactic acid)/graphene oxide-ZnO nanocomposite films with good mechanical, dynamic mechanical, anti-UV and antibacterial properties. J. Chem. Technol. Biotechnol. 90, 1677–1684. https://doi.org/10.1002/jctb.4476
ISO179-1, 2010. Plastics - Determination Of Charpy Impact Properties - Part 1: Non-instrumented Impact Test.
Jiang, L., Zhang, J., Wolcott, M.P., 2007. Comparison of polylactide/nano-sized calcium carbonate and polylactide/montmorillonite composites: Reinforcing effects and toughening mechanisms. Polymer (Guildf). 48, 7632–7644. https://doi.org/10.1016/j.polymer.2007.11.001
K., P., Mohanty, S., Nayak, S.K., 2012. Polylactide/transition metal ion modified montmorillonite nanocomposite-a critical evaluation of mechanical performance and thermal stability. Polym. Compos. 33, 1848–1857. https://doi.org/10.1002/pc.22317
Kontou, E., Georgiopoulos, P., Niaounakis, M., 2012. The role of nanofillers on the degradation behavior of polylactic acid. Polym. Compos. 33, 282–294. https://doi.org/10.1002/pc.21258
Kontou, E., Niaounakis, M., Georgiopoulos, P., 2011. Comparative study of PLA nanocomposites reinforced with clay and silica nanofillers and their mixtures. J. Appl. Polym. Sci. 122, 1519–1529. https://doi.org/10.1002/app.34234
Krikorian, V., Pochan, D.J., 2003. Poly (L-Lactic Acid)/Layered Silicate Nanocomposite: Fabrication, Characterization, and Properties. Chem. Mater. 15, 4317–4324. https://doi.org/10.1021/cm034369+
Lai, S.M., Wu, S.H., Lin, G.G., Don, T.M., 2014. Unusual mechanical properties of melt-blended poly(lactic acid) (PLA)/clay nanocomposites. Eur. Polym. J. 52, 193–206. https://doi.org/10.1016/j.eurpolymj.2013.12.012
Murariu, M., Dubois, P., 2016. PLA composites: From production to properties. Adv. Drug Deliv. Rev. 107, 17–46. https://doi.org/10.1016/j.addr.2016.04.003
Nur-Aimi, M.N., Anuar, H., 2016. Effect of Plasticizer on Fracture Toughness of Polylactic Acid Reinforced with Kenaf Fibre and Montmorillonite Hybrid Biocomposites, in: Nanoclay Reinforced Polymer Composites. pp. 263–280. https://doi.org/10.1007/978-981-10-0950-1
Park, S.D., Todo, M., Arakawa, K., Koganemaru, M., 2006. Effect of crystallinity and loading-rate on mode i fracture behavior of poly(lactic acid). Polymer (Guildf). 47, 1357–1363. https://doi.org/10.1016/j.polymer.2005.12.046

Pirani, S.I., Krishnamachari, P., Hashaikeh, R., 2013. Optimum loading level of nanoclay in PLA nanocomposites: Impact on the mechanical properties and glass transition temperature. J. Thermoplast. Compos. Mater. 27, 1461–1478. https://doi.org/10.1177/0892705712473627

Pluta, M., Paul, M.A., Alexandre, M., Dubois, P., 2006. Plasticized polylactide/clay nanocomposites. I. The role of filler content and its surface organo-modification on the physico-chemical properties. J. Polym. Sci. Part B Polym. Phys. 44, 299–311. https://doi.org/10.1002/polb.20694

Sinha Ray, S., Yamada, K., Okamoto, M., Fujimoto, Y., Ogami, A., Ueda, K., 2003. New polylactide/layered silicate nanocomposites. 5. Designing of materials with desired properties. Polymer (Guildf). 44, 6633–6646. https://doi.org/10.1016/j.polymer.2003.08.021

Stoclet, G., Lefebvre, J.M., Séguéla, R., Vanmansart, C., 2014. In-situ SAXS study of the plastic deformation behavior of polylactide upon cold-drawing. Polym. (United Kingdom) 55, 1817–1828. https://doi.org/10.1016/j.polymer.2014.02.010